

# Perspective picture from Visual Sphere: *a new approach to image rasterization*

Jakub Maximilian Fober

*April 10, 2020*

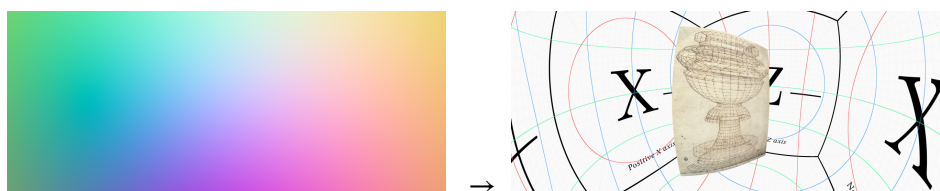


Figure 1: Example of aliasing-free, single-pass rasterization of polygon quad in real-time, from a perspective vector map, where  $\Omega_d = 270^\circ$ ,  $k = 0.32$ ,  $l = 62\%$ ,  $s = 86\%$ .

## Abstract

In this paper alternative method for real-time 3D model rasterization is given. Surfaces are drawn in perspective-map space which acts as a virtual camera lens. It can render single-pass  $360^\circ$  angle of view (AOV) image of unlimited shape, view-directions count and unrestrained projection geometry complexity (e.g. direct lens distortion, projection mapping, curvilinear perspective), natively aliasing-free. In conjunction to perspective vector map, visual-sphere perspective model is proposed. A model capable of combining pictures from sources previously incompatible, like fish-eye camera and wide-angle lens picture. More so, method is proposed for measurement and simulation of a real optical system variable no-parallax point (NPP). This study also explores philosophical and historical aspects of picture perception and presents a guide for perspective design.



---

talk@maxfober.space  
https://maxfober.space  
ORCID iD / 0000-0003-0414-4223

# Contents

<b>Introduction</b>	<b>4</b>
<b>1 on Visual Sphere perspective</b>	<b>4</b>
1.1 Rasterization with perspective map . . . . .	5
1.1.1 Aliasing-free step function . . . . .	6
1.1.2 Miter mask for AA . . . . .	7
1.1.3 Matrix rasterization . . . . .	9
1.1.4 Interpolation in Fragment Shader . . . . .	11
1.1.5 Perspective shader pass . . . . .	13
1.2 Wire-frame rasterization . . . . .	13
1.3 Simple particle rasterization . . . . .	15
1.4 Hidden surface problem . . . . .	16
<b>2 Perspective picture transformations</b>	<b>17</b>
2.1 Universal perspective . . . . .	18
2.1.1 2D–3D transformation . . . . .	18
2.1.2 3D–2D transformation . . . . .	19
2.2 of various projections . . . . .	21
2.2.1 Linear perspective . . . . .	21
2.2.2 Curved panorama . . . . .	22
2.2.3 Full dome . . . . .	23
2.2.4 Equirectangular projection . . . . .	24
2.2.5 Mirror dome projection . . . . .	24
2.2.6 Projection mapping . . . . .	26
2.2.7 Cube-mapping . . . . .	27
2.2.8 Multiple-screen array . . . . .	28
2.2.9 Virtual reality . . . . .	29
2.3 Lens distortions . . . . .	30
<b>3 Variable NPP</b>	<b>30</b>
<b>4 Appendix</b>	<b>31</b>
4.1 Symbolic picture . . . . .	33
4.2 Visual Sphere . . . . .	34
4.2.1 azimuthal projections . . . . .	34
4.3 Motion and perspective . . . . .	35
4.3.1 Attention focusing . . . . .	36
4.3.2 in motion . . . . .	37
4.4 History of the topic . . . . .	38
<b>5 Conclusion</b>	<b>40</b>
<b>References</b>	<b>45</b>

## List of Figures

1	Rasterized polygon example . . . . .	1
2	Visual sphere model . . . . .	5
3	Visual sphere coordinates . . . . .	6
4	Aliasing-free step function . . . . .	7
5	Rasterization masks in RGB . . . . .	9
6	Barycentric coordinates in RGB . . . . .	11
7	Simple particle model . . . . .	15
8	Mirror dome projection . . . . .	25
9	Radial compression charts . . . . .	32
10	Motion in various azimuthal projections . . . . .	36
11	View orientation and perspective . . . . .	38
12	Anamorphic lens picture example . . . . .	39
13	Rasterization examples . . . . .	41
14	Vertex rasterization process flowchart . . . . .	42
15	Fragment rasterization process flowchart . . . . .	43
16	Floating no-parallax point . . . . .	44

## Listings

1	Pixel step function . . . . .	7
2	Miter mask for aliasing-free raster . . . . .	8
3	Smooth rasterization . . . . .	10
4	Jagged rasterization . . . . .	10
5	Barycentric interpolation vector . . . . .	12
6	Smooth wireframe . . . . .	14
7	Jagged wireframe . . . . .	14
8	Particle rasterization . . . . .	16
9	Universal-perspective map . . . . .	19
10	Rectilinear map . . . . .	21
11	Curved panorama map . . . . .	22
12	Full dome map . . . . .	23
13	Equirectangular map . . . . .	24
14	Mirror dome map . . . . .	25
15	Projection-mapping map . . . . .	27
16	Horizontal screen array map . . . . .	28
17	Virtual reality map . . . . .	29
18	Lens distortion . . . . .	30

## Introduction

There is a great demand for perspective projection model able to produce computer-generated (CG) image up to  $360^\circ$  of view, with lens-distortions, directly from three-dimensional space, to pixel data. Currently there is no practical direct method for rasterization of real-time graphics in curvilinear perspective.<sup>19</sup> Every real-time perspective imagery incorporates *Pinhole Camera* model as a base, some with additional layers of distortion on top. Also knowledge about relationship between motion and perspective has not been properly formulated, leaving a void in that field of image science. This paper aims at solving those issues. Study presents new, universal model for perspective projection and rasterization in CG graphics. It also explores history of perspective picture, redefines abstract theorem of image (as recorded in common-knowledge) and establishes rules for picture's perspective design.

This paper begins with brief introduction to the visual-sphere perspective and starts with details about rasterization. If one is not familiar to the terms and topic, Appendix on page 31 gives introduction and basic knowledge as well as brief history in the topic of perspective and picture perception. Section 2 on page 17 presents algorithms for producing various perspective maps used in visual-sphere rasterization. Within that, subsection 2.1 on page 18 presents *Universal Perspective* model. It can describe variable image geometry in common projections. Section 3 on page 30 overview measurement approach and image rendering technique for variable no-parallax point of real optical systems. Additional figures are presented at the end of document.

## 1 From Visual Pyramid to Visual Sphere

Visual pyramid of ALBERTI theorem is by definition limited to acute angles, which is restricting in terms of projections it can describe. This property makes stitching or layering multiple pictures defined in such space a problematic task. In standard perspective model 3D point position is transformed into 2D screen coordinates. But in a case of some curvilinear projections, points are stretched into lines, like equidistant projection, where at  $\Omega = 360^\circ$  point opposite to the camera view direction forms a ring around picture bounds. In proposed visual sphere model, every point in perspective picture has its own spherical coordinate. Thus single point on a sphere can occupy multiple places in the picture, conforming to the principles of curvilinear perspective. Such perspective format allows for stitching and layering images of any single-point projection geometry.

*Remark.* Visual sphere image can be emulated from six visual-pyramid pictures, each covering  $\Omega = 90^\circ$ , with three mutually perpendicular and three adjacent camera view directions.<sup>a</sup>

---

<sup>a</sup>Process known as *cube mapping*



operations.

$$\vec{G}'_1 = \hat{G} \cdot \|\vec{A} \times \vec{B}\| \quad (1)$$

$$\vec{G}'_2 = \hat{G} \cdot \|\vec{B} \times \vec{C}\| \quad (2)$$

$$\vec{G}'_3 = \hat{G} \cdot \|\vec{C} \times \vec{A}\| \quad (3)$$

$$\overline{ABC} \mapsto G = \text{step}(\vec{G}'_1) \wedge \text{step}(\vec{G}'_2) \wedge \text{step}(\vec{G}'_3) \quad \blacksquare \quad (4)$$

Rotation of perspective map vector  $\hat{G}$  is performed by a dot product between each  $\hat{G}$  and rotation-direction vector. This is a dot product between perspective map  $G$  and normalized cross product of two edge points. Rotation vector doesn't have to be normalized, but that could cause some precision errors, especially when using aliasing-free step function.

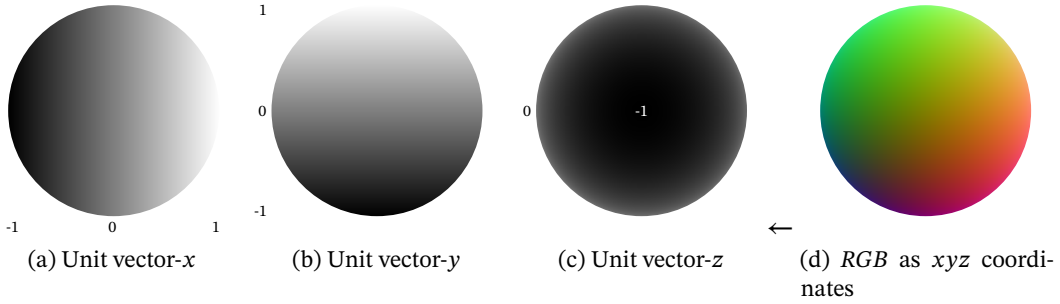


Figure 3: Visual sphere in vector coordinates as seen from outside facing  $Z$  direction. Each vector component  $x$ ,  $y$  and  $z$  can be rotated independently.

Visual sphere perspective model is ultimately a *cosine*-based perspective model and can produce pictures in both *tangent perspective* and *sine perspective*. As seen in figure 3, each sphere surface point has a value associated to its position. Those three values also represent cosine of an angle between axis vectors  $[1, 0, 0]$ ,  $[0, 1, 0]$ ,  $[0, 0, 1]$  and the surface position vector. After rotation of  $\hat{G}$ , those three axes are represented by rotation matrix vectors.

### 1.1.1 Aliasing-free step function

Step function is performed on rotated  $\vec{G}'$  coordinates and determines inside and outside of a polygon for each edge. Aliasing-free result can be achieved by making step-function's slope not binary, but pixel-wide (see figure 4 on the following page). Below presented are two algorithms for a step function.

$$\text{pstep}(g) = \left( \frac{g}{\Delta(g)} + \frac{1}{2} \right) \cap [0, 1] \quad (5)$$

$$\text{bstep}(g) = \begin{cases} 1, & \text{if } g > 0 \\ 0, & \text{otherwise} \end{cases} \quad (6)$$

$\text{pstep}(g)$  function ( $p$  standing for *pixel*) gives smooth aliasing-free result. The  $\text{bstep}(g)$  is a binary operation and gives aliased output.  $\Delta(x)$  function is equivalent of the ***fwidth***( $x$ ) function. The  $1/2$  offset centers gradient at the polygon edge as seen in subfigure 4c compared to 4a.

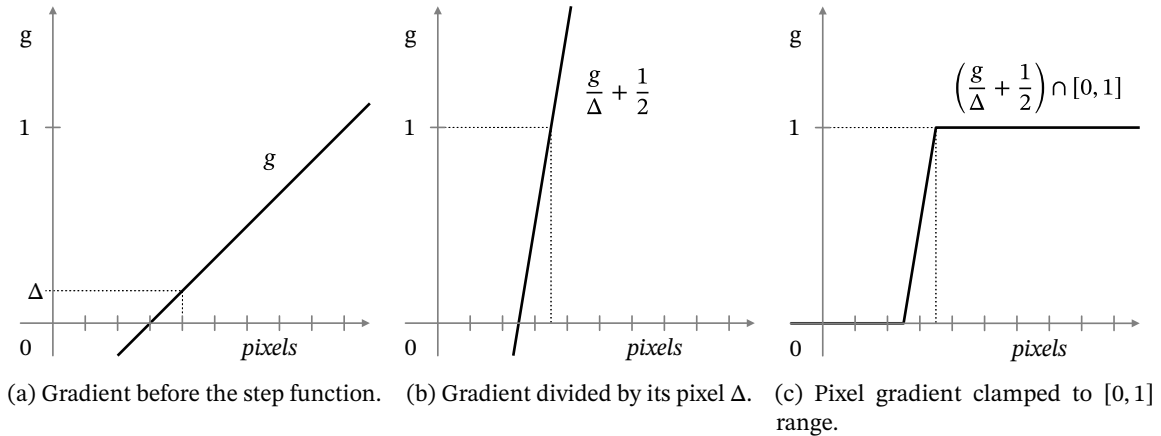


Figure 4: Aliasing-free step function process, where  $g$  is the gradient function,  $\Delta$  is equivalent to  $\text{fwidth}(g)$  function. Horizontal axis represents pixel position and vertical-axis the value of  $g$ .

```
1 | float pxstep(float scalar)
2 | { return clamp(scalar / fwidth(scalar) + 0.5, 0.0, 1.0); }
```

Listing 1: Aliasing-free step function in GLSL.

*Remark.* When combining polygons into polygon-strip using pixel-step function, it is important to sum each mask, otherwise visible seam may occur.

### 1.1.2 Miter mask for pixel-step rasterization

In special case, when projected polygon's edges meet at very shallow angle, corers will extend beyond polygon's outline (due to half-pixel offset in the  $\text{pstep}(g)$  function). This is corrected by a miter mask. There are many ways to calculate such mask, one is to define the smallest circle over projected triangle. Following algorithm uses barycentric coordinates to determine the smallest circle center and size.<sup>10</sup>

$$a^2 = |\hat{B} - \hat{C}|^2 = (\hat{B} - \hat{C}) \cdot (\hat{B} - \hat{C}) \quad (7)$$

$$b^2 = |\hat{C} - \hat{A}|^2 = (\hat{C} - \hat{A}) \cdot (\hat{C} - \hat{A}) \quad (8)$$

$$c^2 = |\hat{A} - \hat{B}|^2 = (\hat{A} - \hat{B}) \cdot (\hat{A} - \hat{B}) \quad (9)$$

$$\begin{bmatrix} \vec{O}_s \\ \vec{O}_t \\ \vec{O}_p \end{bmatrix} = \begin{bmatrix} a^2(b^2 + c^2 - a^2) \\ b^2(c^2 + a^2 - b^2) \\ c^2(a^2 + b^2 - c^2) \end{bmatrix} \quad (10)$$

$$\vec{S} = \begin{cases} 0.5(\hat{B} + \hat{C}), & \text{if } \vec{O}_s \leq 0 \\ 0.5(\hat{C} + \hat{A}), & \text{if } \vec{O}_t \leq 0 \\ 0.5(\hat{A} + \hat{B}), & \text{if } \vec{O}_p \leq 0 \\ \frac{\vec{O}_s \hat{A} + \vec{O}_t \hat{B} + \vec{O}_p \hat{C}}{\vec{O}_s + \vec{O}_t + \vec{O}_p}, & \text{otherwise} \end{cases} \quad (11) \quad \blacksquare$$

Where  $\vec{O}$  is the barycentric coordinate of circumcenter.  $a^2, b^2, c^2$  are squared lengths of projected triangle's edges.  $\vec{S}$  is the smallest-circle center vector which length is equal to the cosine of an angle between  $\vec{S}$  and the smallest-circle rim. Polygon triangle is degenerate if  $0 = \vec{O}_s + \vec{O}_t + \vec{O}_p$ , meaning all projected  $\hat{A}, \hat{B}, \hat{C}$  points lay in line. In such case miter mask can be omitted.

```

1 float dot(vec3 vector) { return dot(vector, vector); }
2
3 // Once per polygon
4 vec4 getMiterVector(mat3 triangle)
5 {
6     // Project polygon onto sphere
7     triangle[0] = normalize(triangle[0]); // Vertex A
8     triangle[1] = normalize(triangle[1]); // Vertex B
9     triangle[2] = normalize(triangle[2]); // Vertex C
10
11     // Get polygon sides squared
12     vec3 barycenter = vec3(
13         dot(triangle[1]-triangle[2]),
14         dot(triangle[2]-triangle[0]),
15         dot(triangle[0]-triangle[1])
16     );
17     // Get circumcenter
18     barycenter *= barycenter.gbr+barycenter.brg-barycenter;
19     // Get smallest circle vector
20     if (barycenter.s <= 0.0)
21         barycenter = 0.5*(triangle[1]+triangle[2]);
22     else if (barycenter.t <= 0.0)
23         barycenter = 0.5*(triangle[2]+triangle[0]);
24     else if (barycenter.p <= 0.0)
25         barycenter = 0.5*(triangle[0]+triangle[1]);
26     else

```

```

27 |         barycenter = ( barycenter . s * triangle [ 0 ]
28 |                       + barycenter . t * triangle [ 1 ]
29 |                       + barycenter . p * triangle [ 2 ] )
30 |                       / ( barycenter . s + barycenter . t + barycenter . p );
31 |
32 |     return vec4 ( normalize ( barycenter ) , length ( barycenter ) );
33 | }

```

Listing 2: Polygon miter mask function in GLSL, where matrix *triangle* represents vertices in camera-space.

Having the smallest circle center vector  $\vec{S}$ , rasterization algorithm can be updated as follows:

$$\vec{G}'_1 = \hat{G} \cdot \|\vec{A} \times \vec{B}\| \quad (12)$$

$$\vec{G}'_2 = \hat{G} \cdot \|\vec{B} \times \vec{C}\| \quad (13)$$

$$\vec{G}'_3 = \hat{G} \cdot \|\vec{C} \times \vec{A}\| \quad (14)$$

$$\vec{G}'_4 = \hat{G} \cdot \hat{S} - |\vec{S}| \quad (15)$$

$$\overline{ABC} \mapsto G = \text{pstep}(\vec{G}'_1) \wedge \text{pstep}(\vec{G}'_2) \wedge \text{pstep}(\vec{G}'_3) \wedge \text{pstep}(\vec{G}'_4) \quad \blacksquare \quad (16)$$

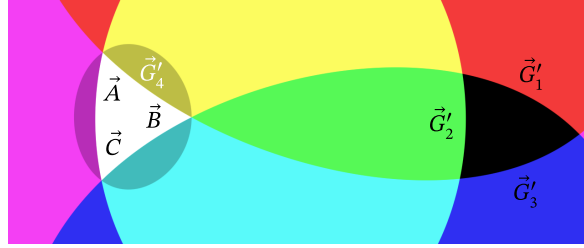


Figure 5: Rasterization masks as RGB values, where perspective map represents  $\Omega_d = 270^\circ$ ,  $k = 0.32$ ,  $l = 62\%$ ,  $s = 86\%$ .

### 1.1.3 Rasterization using matrix multiplication

Since rasterization involves multiple dot products, part of the process can be mitigated to matrix multiplication, where each matrix row represents rotation vector. Such matrix is calculated once per polygon, per frame and executed per fragment pixel. Full vertex rasterization process is presented on figure 14 on page 42.

$$\begin{bmatrix} \vec{G}'_1 \\ \vec{G}'_2 \\ \vec{G}'_3 \\ \vec{G}'_4 \end{bmatrix} = \begin{bmatrix} \hat{G}_x \\ \hat{G}_y \\ \hat{G}_z \end{bmatrix} \begin{bmatrix} \|\vec{A} \times \vec{B}\| \\ \|\vec{B} \times \vec{C}\| \\ \|\vec{C} \times \vec{A}\| \\ \hat{S}_x \hat{S}_y \hat{S}_z \end{bmatrix} - \begin{bmatrix} 0 \\ 0 \\ 0 \\ |\vec{S}| \end{bmatrix} \quad (17)$$

$$\overline{ABC} \mapsto G = \text{pstep}(\vec{G}'_1) \wedge \text{pstep}(\vec{G}'_2) \wedge \text{pstep}(\vec{G}'_3) \wedge \text{pstep}(\vec{G}'_4) \quad \blacksquare \quad (18)$$

```

1  vec3 normal(vec3 A, vec3 B)
2  { return normalize(cross(A, B) ); }
3
4  // Once per polygon
5  mat3 getRasterMatrix(mat3 triangle)
6  {
7      return mat3(
8          normal(triangle[0], triangle[1]),
9          normal(triangle[1], triangle[2]),
10         normal(triangle[2], triangle[0])
11     );
12 }
13
14 // Once per fragment pixel
15 float getPolygonOutline(vec3 visual_sphere, mat3 raster,
16     vec4 miter)
17 {
18     vec4 masks;
19     masks.rgb = visual_sphere*raster;
20     masks.a = dot(visual_sphere, miter.xyz)-miter.w;
21
22     float outline = pxstep(masks[0]);
23     for (int i=1; i<4; i++)
24         outline *= pxstep(masks[i]);
25
26     return outline;
27 }

```

Listing 3: Aliasing-free rasterization function in GLSL. Function `pxstep()` is described in listing 1 on page 7.

```

1  // Once per region
2  bool getPolygonRegion(vec3 visual_sphere, mat3 raster)
3  {
4      vec3 masks = visual_sphere*raster;
5      // extend outline
6      masks += fwidth(masks)*0.5;
7
8      bool outline = masks[0]>0.0;
9      for (int i=1; i<4; i++)
10         outline &= masks[i]>0.0;
11
12     return outline;
13 }

```

Listing 4: Binary (jagged) step rasterization function in GLSL. This version produces aliased result, suitable for low-resolution fragment region evaluation.

This procedure can be expanded to any convex  $n$ -sided planar polygon using procedural equation as follows:

$$\begin{bmatrix} \vec{G}'_1 \\ \vec{G}'_2 \\ \vdots \\ \vec{G}'_n \end{bmatrix} = \begin{bmatrix} \hat{G}_x \\ \hat{G}_y \\ \hat{G}_z \end{bmatrix} \begin{bmatrix} \|T_1 \times T_2\| \\ \|T_2 \times T_3\| \\ \vdots \\ \|T_n \times T_{(i+1) \bmod n}\| \end{bmatrix} \quad (19)$$

$$\text{mask}(\vec{G}') = \prod_{i=1}^n \text{step}(\vec{G}'_i) \quad \blacksquare \quad (20)$$

Where  $T$  describes  $n$ -sided polygon points  $n \times 3$  matrix, where each row represents vertex position (counting clock-wise). Each rotation vector is derived from cross product between  $i$ -vertex and  $i + 1$  (next one going clock-wise). For the the last  $n^{\text{th}}$  vertex, next one is  $N\circ 1$ .

#### 1.1.4 Fragment data interpolation from barycentric coordinates

Rendering realistic polygon graphics involves shading and texture mapping. Values of normal, depth and UV coordinates associated to each vertex are interpolated across polygon surface using barycentric coordinates of the fragment point.

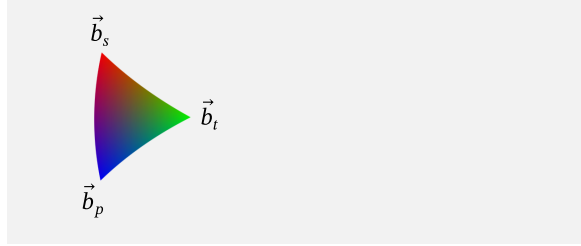


Figure 6: Barycentric coordinates as RGB values, where perspective map represents  $\Omega_d = 270^\circ$ ,  $k = 0.32$ ,  $l = 62\%$ ,  $s = 86\%$ .

$$\vec{N} = (\vec{A} - \vec{B}) \times (\vec{C} - \vec{B}) \quad (21)$$

$$= (\vec{B} - \vec{C}) \times (\vec{A} - \vec{C}) \quad (22)$$

$$= (\vec{C} - \vec{A}) \times (\vec{B} - \vec{A}) \quad (23)$$

Normal vector  $\vec{N} \in \mathbb{R}^3$  of the triangle plane  $\overline{ABC}$  is derived from cross product of two triangle edges. Length of this vector is equal to the area of a parallelogram formed by those two edges, which is equal to double the area of triangle  $\overline{ABC}$ .

$$r = \frac{\vec{A} \cdot \vec{N}}{\hat{G} \cdot \vec{N}} = \frac{\vec{B} \cdot \vec{N}}{\hat{G} \cdot \vec{N}} = \frac{\vec{C} \cdot \vec{N}}{\hat{G} \cdot \vec{N}} \quad (24)$$

$$\equiv |\hat{G} \rightarrow \overline{ABC}| \quad (25)$$

Distance  $r$  represents multiplier of the visual sphere vector  $\hat{G}$ , to intersection point on the  $ABC$  triangle plane. Since  $\hat{G}$  is a unit vector, value  $r$  can be exported as depth (representing distance, not  $z$ -buffer). Here vector  $\vec{A}, \vec{B}, \vec{C}$  in the numerator can be replaced by any point on the triangle plane.

$$\begin{bmatrix} \vec{b}_s \\ \vec{b}_t \\ \vec{b}_p \end{bmatrix} = \begin{bmatrix} |(\vec{B} - r\hat{G}) \times (\vec{C} - r\hat{G})| \\ |(\vec{C} - r\hat{G}) \times (\vec{A} - r\hat{G})| \\ |(\vec{A} - r\hat{G}) \times (\vec{B} - r\hat{G})| \end{bmatrix} \div |\vec{N}| \quad (26)$$

Since  $\vec{A} \cdot \vec{B} = |\vec{A}||\vec{B}| \cos \alpha$  and  $\overline{AB} \perp (\vec{A} \times \vec{B})$  this equation can be rewritten using triple product, as follows.

$$\begin{bmatrix} \vec{b}_s \\ \vec{b}_t \\ \vec{b}_p \end{bmatrix} = \begin{bmatrix} (\vec{C} - r\hat{G}) \times (\vec{B} - r\hat{G}) \cdot \vec{N} \\ (\vec{A} - r\hat{G}) \times (\vec{C} - r\hat{G}) \cdot \vec{N} \\ (\vec{B} - r\hat{G}) \times (\vec{A} - r\hat{G}) \cdot \vec{N} \end{bmatrix} \div (\vec{N} \cdot \vec{N}) \quad (27)$$

```

1  vec3 dot(vec3 vector) { return dot(vector, vector); }
2
3  // Once per polygon
4  vec3 getHardNormal(mat3 triangle)
5  { return cross(triangle[0]-triangle[1],
6             triangle[2]-triangle[1]); }
7
8  // Once per fragment pixel
9  vec4 getBarCoord(vec3 visual_sphere, mat3 triangle, vec3
10 hard_normal)
11 {
12     // Extend onto polygon plane intersection
13     float depth = dot(triangle[0], hard_normal)
14     /dot(visual_sphere, hard_normal);
15     visual_sphere *= depth;
16
17     for (int i=0; i<3; i++)
18         triangle[i] -= visual_sphere;
19
20     return vec4(vec3(
21         dot(cross(triangle[2], triangle[1]), hard_normal),
22         dot(cross(triangle[0], triangle[2]), hard_normal),
23         dot(cross(triangle[1], triangle[0]), hard_normal)
24     )/dot(hard_normal), depth);

```

Listing 5: Barycentric vector function with hard normal and depth functions for fragment-data interpolation in GLSL.

Barycentric vector  $\vec{b}$  is a proportion of surface area. From vector  $\vec{b}$ , various vertex properties can be interpolated (e.g. depth, normal vector and texture coordinates), given each vertex  $A, B$  and  $C$  has associated value.

$$f_r = r \quad (28)$$

$$f_{\vec{N}} = \|\vec{b}_s A_{\vec{N}} + \vec{b}_t B_{\vec{N}} + \vec{b}_p C_{\vec{N}}\| \quad (29)$$

$$f_{\vec{f}} = \vec{b}_s A_{\vec{f}} + \vec{b}_t B_{\vec{f}} + \vec{b}_p C_{\vec{f}} \quad (30)$$

Interpolation of fragment data  $f$  is done through a dot product between barycentric coordinate vector  $\vec{b}$  and values associated to each vertex. Here  $f_r$  is the depth pass (representing distance, not z position),  $f_{\vec{N}}$  is the interpolated normal vector and  $f_{\vec{f}}$  are the texture coordinates. All interpolations are perspective-correct. Figure 15 on page 43 shows this process in a step-by-step flowchart.

### 1.1.5 Perspective pixel-shader pass

Prior to geometry rasterization, pixel perspective shader pass may be performed. Its output is a perspective vector map texture. This pipeline addition enables special effects like dynamic perspective and projection mapping, flat mirror reflection, screen-space refraction (e.g. concave refractive surfaces which expand AOV), etc.

*Example.* Projection mapping with dynamic view-position can be achieved by transforming vector data of world-position-pass texture  $S$ . Knowing viewer position  $\vec{O}$ , offset can be applied to  $\vec{S}$ . When normalized,  $\hat{S}'$  produces perspective map vector  $\hat{G} = \|\vec{S} - \vec{O}\|$ . Complexity of projection surface and number of views (used projectors) is outside of concern, as view-position transformation is performed on a baked texture. Exact formula for projection mapping is available in sub-subsection 2.2 on page 21.

## 1.2 Wire-frame line segment rasterization

It is possible to produce screen-relative-thick line drawing based on a perspective map. Following algorithm will produce wire-frame image of projected  $\overline{AB}$  line segment.

$$\vec{G}'_z = \hat{G} \cdot \|\vec{A} \times \vec{B}\| \quad (31)$$

Perspective vector map component  $\hat{G}_z$  is rotated by  $\overline{ABO}$  tangent vector  $\|\vec{A} \times \vec{B}\|$ , where  $\vec{O}$  is the observation point.

$$\text{blstep}(\vec{G}'_z) = \begin{cases} 1, & \text{if } \Delta(\vec{G}'_z) - |2\vec{G}'_z| > 0 \\ 0, & \text{otherwise} \end{cases} \quad (32)$$

$$\text{plstep}(\vec{G}'_z) = 1 - \min\left(\frac{|\vec{G}'_z|}{\Delta(\vec{G}'_z)}, 1\right) \quad (33)$$

Line step function in two versions, binary (aliased) and pixel-smooth (aliasing-free).  $\Delta(x)$  is equivalent to **fwidth**( $x$ ) function.

$$\vec{L} = \frac{\hat{A} + \hat{B}}{2} \quad (34)$$

$$h = \text{lstep}(\vec{G}'_z) \quad (35)$$

$$l = h \wedge \text{step}(\hat{G} \cdot \hat{L} - |\vec{L}|) \quad \blacksquare \quad (36)$$

Radial mask combined with great circle  $h$  forms  $\overline{AB}$  line segment image  $l$ .  $\hat{L}$  is the line-middle vector,  $\text{lstep}(\vec{G}'_z)$  function rasterizes great-circle  $h$ . Radial mask is formed by the step( $x$ ) function of dot product between perspective map vector  $\hat{G}$  and line-middle vector  $\hat{L}$ , minus  $|\vec{L}| = \cos \theta/2$ .

```

1 float lpxstep(float scalar)
2 { return 1.0 - min(abs(scalar) / fwidth(scalar), 1.0); }
3
4 // Once per polygon side
5 vec4 getLineVector(vec3 A, vec3 B)
6 {
7     // Project vertices onto sphere
8     A = normalize(A); B = normalize(B);
9     vec3 line_center = (A+B)*0.5;
10    return vec4(normalize(line_center),
11               length(line_center) );
12 }
13
14 // Once per polygon side
15 float normal(vec3 A, vec3 B)
16 { return normalize(cross(A, B) ); }
17
18 // Once per line's pixel
19 float getLineSegment(vec3 visual_sphere, vec3 normal, vec4
20                      line_vec)
21 {
22     // Great circle
23     float line = lpxstep(dot(visual_sphere, normal) );
24     // Apply segment mask
25     return line * pxstep(dot(visual_sphere, line_vec.xyz) -
26                          line_vec.w);

```

Listing 6: Aliasing-free line segment rasterization function in GLSL. Function `pxstep()` can be found in listing 1 on page 7.

```

1 // Once per line's pixel
2 bool getAliasedLineSegment(vec3 visual_sphere, vec3 normal,
3                             vec3 line_vec)

```

```

4 |   float great_circle = dot(visual_sphere , normal);
5 |   // Binary line-step operation
6 |   bool line = fwidth(great_circle)-abs(2.0*great_circle) >
   |             0.0;
7 |   // Apply segment mask
8 |   return line && dot(visual_sphere , line_vec.xyz)-line_vec
   |             .w > 0.0;
9 | }

```

Listing 7: Binary (jagged) line segment rasterization function in GLSL.

### 1.3 Simple procedural particle rasterization

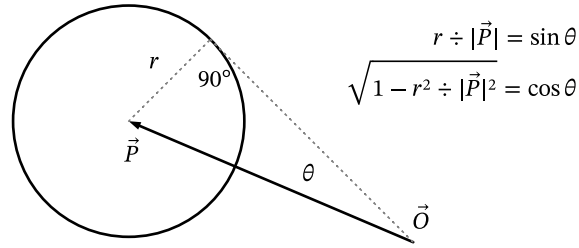


Figure 7: Simple particle model, where  $r$  is the particle radius and  $\vec{P}$  is the particle position from observation point  $\vec{O}$ .

Following algorithm will produce mask image of spherical particle of given position and radius.

$$\text{particle}(\hat{G}, \vec{P}, r) = \text{step}\left(\hat{G} \cdot \hat{P} - \sqrt{1 - r^2 \div (\vec{P} \cdot \vec{P})}\right) \quad (37)$$

Where  $\vec{P} \in \mathbb{R}^3$  is the particle position,  $r$  is particle radius and  $\hat{G}$  is the perspective map vector. To obtain texture coordinates within the particle, following algorithm can be used.

$$\hat{X} = \|\vec{P}_z, 0, -\vec{P}_x\| \quad (38)$$

$$\hat{Y} = \|\hat{X} \times \vec{P}\| \equiv \hat{X} \times \hat{P} \quad (39)$$

$$\begin{bmatrix} \vec{f}_s^P \\ \vec{f}_t^P \end{bmatrix} = \begin{bmatrix} \hat{G}_x \\ \hat{G}_y \\ \hat{G}_z \end{bmatrix} \begin{bmatrix} \hat{X}_x & \hat{X}_y & \hat{X}_z \\ \hat{Y}_x & \hat{Y}_y & \hat{Y}_z \end{bmatrix} \frac{|\vec{P}|}{2r} + \frac{1}{2} \quad \blacksquare \quad (40)$$

Where  $\vec{f}^P$  is the texture coordinate of the particle,  $\hat{X}$  and  $\hat{Y}$  are rotation matrix vectors. Full particle rasterization process, with texture coordinates and round mask can be described as following algorithm.

$$\begin{bmatrix} \vec{G}'_1 \\ \vec{G}'_2 \\ \vec{G}'_3 \end{bmatrix} = \begin{bmatrix} \hat{G}_x \\ \hat{G}_y \\ \hat{G}_z \end{bmatrix} \begin{bmatrix} \|\vec{P}_z, 0, -\vec{P}_x\| \\ \|\vec{P}_z, 0, -\vec{P}_x\| \times \hat{P} \\ \hat{P}_x \quad \hat{P}_y \quad \hat{P}_z \end{bmatrix} \quad (41)$$

$$m^P = \text{step} \left( \vec{G}'_3 - \sqrt{1 - r^2 \div (\vec{P} \cdot \vec{P})} \right) \quad \blacksquare \quad (42)$$

$$\begin{bmatrix} \vec{f}_s^P \\ \vec{f}_t^P \end{bmatrix} = \begin{bmatrix} \vec{G}'_1 \\ \vec{G}'_2 \end{bmatrix} \frac{|\vec{P}|}{2r} + \frac{1}{2} \quad \blacksquare \quad (43)$$

Where  $\vec{f}^P \in [0, 1]^2$  are the texture coordinates,  $m^P \in [0, 1]$  is the particle mask,  $\vec{P}$  is the particle position with  $r$  as radius.  $\hat{G}$  is the perspective-map vector.

```

1 float dot(vec3 vector) { return dot(vector, vector); }
2 float sq(float scalar) { return scalar*scalar; }
3 vec3 normal(vec3 A, vec3 B)
4 { return normalize(cross(A, B) ); }
5
6 // Once per particle's pixel
7 float getParticleMask(vec3 visual_sphere, vec4 particle)
8 {
9     return pxstep(dot(visual_sphere, particle.xyz)
10        -sqrt(1.0-sq(particle.w)/dot(particle.xyz) ) );
11 }
12
13 // Once per particle, per frame
14 mat2x3 getPatricleTexCoordMatrix(vec4 particle)
15 {
16     vec3 X = normalize(vec3(particle.z, 0.0, -particle.x) );
17     return mat2x3(X, normal(X, particle.xyz) );
18 }
19
20 // Once per particle's pixel
21 vec2 getParticleTexCoord(vec3 visual_sphere, mat2x3
    particle_mat, vec4 particle)
22 { return (visual_sphere*particle_mat)*length(particle.xyz)/
    particle.w*0.5+0.5; }

```

Listing 8: Particle rasterization function in GLSL. Function pxstep() can be found in listing 1 on page 7.

## 1.4 Hidden surface occlusion

One of the key features of 3D polygon rasterization is hidden surface occlusion (HSO). There are many processes for performing HSO, one of which is depth-pass test, where each pixel depth  $r$  is tested against underlying  $r^\perp$  depth value.

This simple technique works well with binary step function (see subsection 1.1.1 on page 6), but produces aliased result.

Aliasing-free rasterization requires data sorting and polygon splitting, like binary space partitioning<sup>12,20</sup> and sorting regions. This approach produces aliasing-free result, without depth-buffer check and can render scene front-to-back. It is well suited as it can utilize  $n$ -sided convex planar polygon rasterization (see subsection 1.1.3 on page 9). Sorting is only performed once in preprocessor. Some problems may arise when integrating none-static objects into the scene or when rendering organic, bone-driven mesh deformations. In second case, sorting may have to occur per deformation frame. This is an open problem for aliasing-free rasterization, yet to be addressed.

## 2 Perspective transformations of 2D/3D data

In this section presented algorithms produce perspective picture from 3D and 2D data. Most of them describe 2D $\rightarrow$ 3D transformation, which produces perspective vector map from texture coordinates, suitable for rasterization.

*Remark.* For a proper transformation, 2D coordinates must be normalized for a given AOV type (e.g. vertical, diagonal or horizontal).

*Example.* For a pixel  $i$  in picture of aspect-ratio 16:9 and horizontal-AOV, coordinates  $(i_x, i_y)$  must be centered and horizontally normalized, so that  $i_x \in [-1, 1]$  and  $i_y \in [-\frac{9}{16}, \frac{9}{16}]$ .

$$\begin{bmatrix} \vec{f}_x \\ \vec{f}_y \end{bmatrix} = \left( 2 \begin{bmatrix} \vec{f}_s \\ \vec{f}_t \end{bmatrix} - 1 \right) \begin{cases} \left[ 1, \frac{1}{a} \right], & \text{if } \Omega \text{ horizontal} \\ \left[ a, 1 \right] \div \sqrt{1 + a^2}, & \text{if } \Omega \text{ diagonal} \\ \left[ a, 1 \right], & \text{if } \Omega \text{ vertical} \\ \left[ a, 1 \right] \frac{3}{4}, & \text{if } \Omega \text{ horizontal } 4 \times 3 \end{cases} \quad (44)$$

View coordinates  $x, y \in [-1, 1]$  from texture coordinates  $s, t \in [0, 1]$ , where  $a$  is the picture aspect ratio and  $\Omega$  is the AOV.

$$\begin{bmatrix} \vec{f}_s \\ \vec{f}_t \end{bmatrix} = \frac{1}{2} + \frac{1}{2} \begin{bmatrix} \vec{f}_x \\ \vec{f}_y \end{bmatrix} \begin{cases} \left[ 1, a \right], & \text{if } \Omega \text{ horizontal} \\ \left[ \frac{1}{a}, 1 \right] \sqrt{1 + a^2}, & \text{if } \Omega \text{ diagonal} \\ \left[ \frac{1}{a}, 1 \right], & \text{if } \Omega \text{ vertical} \\ \left[ \frac{1}{a}, 1 \right] \frac{4}{3}, & \text{if } \Omega \text{ horizontal } 4 \times 3 \end{cases} \quad (45)$$

Texture coordinates  $s, t \in [0, 1]$  from view coordinates  $x, y \in [-1, 1]$ , where  $a$  is the picture aspect ratio and  $\Omega$  is the AOV.

## 2.1 Universal perspective model

Universal perspective model allows for a smooth adjustment of image geometry in accordance to the visible content. Presented two transforms produce *perspective picture* (see definition on page 34). First 2D→3D transformation produces perspective vector in various common projections, which is suitable for generating universal-perspective maps for rasterization.

### 2.1.1 Transformation of 2D→3D coordinates

This transformation produces visual sphere vector map from texture coordinates, that can be later used as an input for perspective map rasterizer.

$$\vec{f}'_x = \begin{cases} 2\vec{f}_s - 1, & \text{if } \Omega_h \\ a(2\vec{f}_s - 1) \div \sqrt{a^2 + 1}, & \text{if } \Omega_d \\ a(2\vec{f}_s - 1), & \text{if } \Omega_v \end{cases} \quad (46)$$

$$\vec{f}'_y = \begin{cases} (2\vec{f}_t - 1) \div a, & \text{if } \Omega_h \\ (2\vec{f}_t - 1) \div \sqrt{a^2 + 1}, & \text{if } \Omega_d \\ 2\vec{f}_t - 1, & \text{if } \Omega_v \end{cases} \quad (47)$$

$$R = \sqrt{\vec{f}'_x{}^2 + l\vec{f}'_y{}^2} \equiv |\vec{f}'_x, l\vec{f}'_y| \quad (48)$$

$$\theta = \begin{cases} \arctan\left(\tan\left(k\frac{\Omega}{2}\right)R\right) \div k, & 0 < k \leq 1 \\ \frac{\Omega}{2}R, & k = 0 \\ \arcsin\left(\sin\left(k\frac{\Omega}{2}\right)R\right) \div k, & 0 > k \geq -1 \end{cases} \quad (49)$$

$$\begin{bmatrix} \hat{v}_x \\ \hat{v}_y \\ \hat{v}_z \end{bmatrix} = \left\| \begin{bmatrix} \vec{f}'_x \\ \vec{f}'_y \\ 1 \end{bmatrix} \begin{bmatrix} \sin(\theta)/R \\ \sin(\theta)/R \\ \cos \theta \end{bmatrix} \div \begin{bmatrix} 1 \\ l(1-s) + s \\ 1 \end{bmatrix} \right\| \blacksquare \quad (50)$$

Picture coordinates are denoted by vector  $\vec{f} \in [0, 1]^2$ ,  $a$  is picture aspect ratio. Transformed 3D coordinates are represented by normalized vector  $\hat{v} \in [-1, 1]^3$ . Scalar  $k$  represents various projection types:

<i>Gnomonic (rectilinear)</i>	$k = 1$
<i>Stereographic</i>	$k = 0.5$
<i>Equidistant</i>	$k = 0$
<i>Equisolid</i>	$k = -0.5$
<i>Orthographic</i>	$k = -1$

Scalar  $l \in (0, 1]$  is the spherical projection factor, where  $l \approx 0$  represents cylindrical projection and  $l = 1$  is spherical projection. Scalar  $s \in [4/5, 1]$  describes anamorphic correction of non-spherical image. For  $s = 1$  or  $l = 1$  there is no anamorphic correction.

```

1  vec2 getViewCoord(vec2 tex_coord , float aspect , int fov_type
2  )
3  {
4      tex_coord.xy = 2.0*tex_coord.st -1.0;
5      switch (fov_type)
6      {
7          default: // horizontal FOV (type 1)
8              tex_coord.y /= aspect;
9              break;
10         case 2: // diagonal FOV (type 2)
11             tex_coord.xy /= length(vec2(aspect , 1.0) );
12         case 3: // vertical FOV (type 3) and type 2 final step
13             tex_coord.x *= aspect;
14             break;
15     }
16 }
17 vec3 getPerspectiveMap(vec2 view_coord , float fov , float k ,
18     float l , float s)
19 {
20     float halfOmega = radians(fov*0.5);
21     float R = length(vec2(view_coord.x , l*view_coord.y) );
22     float theta;
23     if (k>0.0) theta = atan(tan(k*halfOmega)*R)/k;
24     else if (k<0.0) theta = asin(sin(k*halfOmega)*R)/k;
25     else theta = halfOmega*R;
26
27     view_coord.y /= 1*(1.0-s)+s;
28     return normalize(
29         vec3(view_coord*sin(theta)/R, cos(theta) )
30     );
31 }

```

Listing 9: Visual sphere vector  $\hat{v} \in [-1, 1]$  function from texture coordinates  $\vec{f}$  in GLSL, for universal-perspective system.

### 2.1.2 Transformation of 3D→2D coordinates

This transformation is mainly used in a pixel shader, where basic rectilinear projection can be mapped to spherical one.

$$\hat{v} = [\hat{v}_x, \hat{v}_y, \hat{v}_z] \quad (51)$$

$$\theta = \arccos\left(\hat{v}_z \div \sqrt{\hat{v}_x^2 + l\hat{v}_y^2 + \hat{v}_z^2}\right) \quad (52)$$

$$R = \begin{cases} \tan(k\theta) \div \tan\left(k\frac{\Omega}{2}\right), & 0 < k \leq 1 \\ \theta \div \frac{\Omega}{2}, & k = 0 \\ \sin(k\theta) \div \sin\left(k\frac{\Omega}{2}\right), & 0 > k \geq -1 \end{cases} \quad (53)$$

$$\begin{bmatrix} \vec{f}_x \\ \vec{f}_y \end{bmatrix} = \begin{bmatrix} \hat{v}_x \\ \hat{v}_y \end{bmatrix} \frac{R}{\sqrt{\hat{v}_x^2 + l\hat{v}_y^2}} \begin{bmatrix} 1 \\ l(1-s) + s \end{bmatrix} \quad \blacksquare \quad (54)$$

3D coordinates are represented by a normalized vector  $\hat{v} \in [-1, 1]^3$ , where view origin is at position  $[0, 0, 0]$ . Transformed picture coordinates are represented by vector  $\vec{f} \in [-1, 1]^2$ , where image center is at position  $[0, 0]$ . Angle  $\theta$  is between vector  $\hat{v}$  and the Z axis.  $R$  is the normalized distance between projected vector  $\vec{f}$  and the image center, where  $\vec{f} \leftarrow \hat{v}$ . Angle  $\Omega$  is equal to AOV, where  $\Omega_{\max} \in [\rightarrow \pi, 2\pi]$ . Scalar  $k$  represents various projection types:

<i>Gnomonic (rectilinear)</i>	$k = 1$
<i>Stereographic</i>	$k = 0.5$
<i>Equidistant</i>	$k = 0$
<i>Equisolid</i>	$k = -0.5$
<i>Orthographic</i>	$k = -1$

Scalar  $l \in (0, 1]$  is the spherical projection factor, where  $l \approx 0$  represents cylindrical projection and  $l = 1$  represents spherical projection. Scalar  $s \in [4/5, 1]$  describes anamorphic correction of non-spherical image. For  $s = 1$  or  $l = 1$  there is no anamorphic correction. This transformation is a reverse of the universal 2D→3D transform on page 18.

*Remark.* Combination of 3D and 2D transformation can be used to map between two different projections, for example *Stereographic* ↔ *Equidistant*, using two separate projection components,  $k_i$  and  $k_o$  for input and output image.

**In universal perspective model** base projection type is adjusted by the  $k$  component. It manipulates image perception. Cylindrical projection, is adjusted by the  $l$  component. Low  $l$  values should represent view at level (see subfigure 11a on page 38). For roll motion, recommended value for  $l$  is 100% (see subfigure 11b). Anamorphic correction of non-spherical image, driven by the  $s$  component, depends on subject in view. Purpose of the  $s$  scalar is to adjust proportions of the figure-in-focus.

## 2.2 Perspective map algorithms for various projections

Algorithms presented below produce visual sphere vector map in various projections, which can be later used as an input for perspective map rasterizer. Produced vector  $\hat{v} \in [-1, 1]^3$  can be mapped to image range  $[0, 1]^3$  by simple transformation  $\vec{G}' = \frac{\hat{v}+1}{2}$ .

### 2.2.1 Linear perspective map

$$\begin{bmatrix} \hat{v}_x \\ \hat{v}_y \\ \hat{v}_z \end{bmatrix} = \begin{cases} \begin{bmatrix} \|2\vec{f}_s - 1\| \\ \|(2\vec{f}_t - 1) \div a\| \\ \cot \frac{\Omega_h}{2} \end{bmatrix}, & \text{if horizontal } \Omega \\ \begin{bmatrix} \|a(2\vec{f}_s - 1) \div \sqrt{a^2 + 1}\| \\ \|(2\vec{f}_t - 1) \div \sqrt{a^2 + 1}\| \\ \cot \frac{\Omega_d}{2} \end{bmatrix}, & \text{if diagonal } \Omega \\ \begin{bmatrix} \|a(2\vec{f}_s - 1)\| \\ \|2\vec{f}_t - 1\| \\ \cot \frac{\Omega_v}{2} \end{bmatrix}, & \text{if vertical } \Omega \end{cases} \quad (55)$$

Linear perspective map formula, where  $\hat{v}$  is the visual sphere vector,  $\vec{f}$  represents screen coordinates,  $a$  is the screen aspect ratio and  $\Omega$  is the AOV.

```

1  vec3 getRectilinearMap(vec2 tex_coord , float aspect , float
   fov , int fov_type)
2  {
3      vec3 direction = vec3(
4          2.0*tex_coord - 1.0, // map to range [-1,1]
5          1.0 / tan(0.5*radians(fov) )
6      );
7      switch (fov_type)
8      {
9          default: // horizontal FOV (type 1)
10         direction.y /= aspect;
11         break;
12         case 2: // diagonal FOV (type 2)
13         direction.xy /= length(vec2(aspect , 1.0) );
14         case 3: // vertical FOV (type 3) and type 2 final step
15         direction.x *= aspect;
16         break;
17     }
18
19     return normalize(direction);

```

20 | }

Listing 10: Rectilinear perspective visual-sphere vector  $\hat{v}$  from texture coordinates  $\vec{f}$  in GLSL.

### 2.2.2 Curved panorama map

$$a = \frac{\Omega_h}{h} \quad \blacksquare \quad (56)$$

$$\begin{bmatrix} \vec{f}'_x \\ \vec{f}'_y \end{bmatrix} = \begin{bmatrix} \Omega_h \\ h \end{bmatrix} \left( \begin{bmatrix} \vec{f}_s \\ \vec{f}_t \end{bmatrix} - \frac{1}{2} \right) \quad (57)$$

$$\begin{bmatrix} \hat{v}_x \\ \hat{v}_y \\ \hat{v}_z \end{bmatrix} = \begin{bmatrix} \sin \vec{f}'_x \\ \vec{f}'_y \\ \cos \vec{f}'_x \end{bmatrix} \quad \blacksquare \quad (58)$$

Curved panorama perspective-map formula, where  $a$  is the panorama aspect ratio,  $h$  in the display height-to-radius proportion with  $\Omega$  as the AOV. Vector  $\vec{f}$  represents screen coordinates and  $\hat{v}$  is the visual sphere vector.

```
1 float getPanormaAspect(float horizontal_fov, float height)
2 { return radians(horizontal_fov)/height; }
3
4 vec3 getPanoramaMap(vec2 tex_coord, float horizontal_fov,
5   float height)
6 {
7   tex_coord.xy = vec2(horizontal_fov, height)
8     *(tex_coord.st - 0.5);
9
10  return normalize(
11    vec3(
12      sin(tex_coord.x),
13      tex_coord.y,
14      cos(tex_coord.x)
15    )
16  );
}
```

Listing 11: Curved panorama perspective visual-sphere vector  $\hat{v}$  from texture coordinates  $\vec{f}$  in GLSL.

### 2.2.3 Full dome map

$$\begin{bmatrix} \vec{f}'_x \\ \vec{f}'_y \end{bmatrix} = \begin{bmatrix} 2\vec{f}'_s - 1 \\ 1 - 2\vec{f}'_t \end{bmatrix} \quad (59)$$

$$\theta = |\vec{f}'| \left( \Omega + \frac{\pi}{2} \right) \quad (60)$$

$$\begin{bmatrix} \hat{v}_x \\ \hat{v}_y \\ \hat{v}_z \end{bmatrix} = \begin{bmatrix} \vec{f}'_x \sin \theta \div |\vec{f}'| \\ \cos \theta \\ \vec{f}'_y \sin \theta \div |\vec{f}'| + o \end{bmatrix} \begin{bmatrix} 1 & 0 & 0 \\ 0 & \cos \varphi & -\sin \varphi \\ 0 & \sin \varphi & \cos \varphi \end{bmatrix} \quad \blacksquare \quad (61)$$

$$m = \frac{1 - |\vec{f}'|}{\Delta(1 - |\vec{f}'|)} \cap [0, 1] \quad \blacksquare \quad (62)$$

Full dome perspective-map formula, where  $\vec{f}$  is the screen coordinates vector,  $\Omega$  is the compression angle,  $\varphi$  is the tilt angle,  $\hat{v}$  represents visual sphere vector,  $o$  is the view position offset (in radius) and  $m$  is the radial mask with  $\Delta(x)$  being the equivalent of `fwidth(x)` function.

```

1  vec4 getDomeMap(vec2 tex_coord , float compression , float
    tilt , float offset)
2  {
3      tex_coord.xy = vec2(
4          2.0*tex_coord.s-1.0,
5          1.0-2.0*tex_coord.t
6      );
7      float R = length(tex_coord);
8      float theta = R*radians(compression+90.0);
9
10     vec4 perspective_map = vec4(
11         tex_coord*sin(theta)/R,
12         cos(theta),
13         1.0-R
14     ).xzyw;
15     perspective_map.a = clamp(perspective_map.a
16         /fwidth(perspective_map.a), 0.0, 1.0);
17
18     perspective_map.z += offset;
19     perspective_map.xyz = normalize(perspective_map.xyz);
20
21     tilt = radians(tilt);
22     vec2 rotation = vec2(sin(tilt), cos(tilt) );
23     perspective_map.xyz *= mat3(
24         vec3(1.0,          0.0,          0.0),
25         vec3(0.0, rotation[1], -rotation[0]),
26         vec3(0.0, rotation[0],  rotation[1])
27     );
28
29     return perspective_map;

```

30 | }

Listing 12: Full dome visual-sphere vector  $\hat{v}$  from texture coordinates  $\vec{f}$  in GLSL.

#### 2.2.4 Equirectangular projection map

$$\begin{bmatrix} \vec{f}'_x \\ \vec{f}'_y \end{bmatrix} = \pi \begin{bmatrix} 2\vec{f}_s - 1 \\ \vec{f}_t \end{bmatrix} \quad (63)$$

$$\begin{bmatrix} \hat{v}_x \\ \hat{v}_y \\ \hat{v}_z \end{bmatrix} = \begin{bmatrix} \sin \vec{f}'_x \\ -1 \\ \cos \vec{f}'_x \end{bmatrix} \begin{bmatrix} \sin \vec{f}'_y \\ \cos \vec{f}'_y \\ \sin \vec{f}'_y \end{bmatrix} \quad \blacksquare \quad (64)$$

Equirectangular projection perspective-map formula, where  $\vec{f}$  represents screen coordinates and  $\hat{v}$  is the visual sphere vector.

```

1  vec3 getEquirectangularMap(vec2 tex_coord)
2  {
3      tex_coord.x = 2.0*tex_coord.s-1.0;
4      tex_coord.xy *= radians(180.0);
5
6      vec2 sine = sin(tex_coord);
7      vec2 cosine = cos(tex_coord);
8
9      return vec3(sine.x*sine.y, -cosine.y, cosine.x*sine.y);
10 }
```

Listing 13: Equirectangular projection visual-sphere vector  $\hat{v}$  from texture coordinates  $\vec{f}$  in GLSL.

#### 2.2.5 Mirror dome projection map

*Remark.* Mirror dome projection system was originally developed by P. BOURKE.<sup>5</sup>

$$\vec{I} = \hat{N} - \vec{P} \quad (65)$$

$$\hat{R} = \frac{\vec{I} - 2(\vec{I} \cdot \hat{N})\hat{N}}{|\vec{I} - 2(\vec{I} \cdot \hat{N})\hat{N}|} \quad (66)$$

$$r = \hat{R} \cdot (\vec{O} - \hat{N}) \quad (67)$$

$$r' = r + \sqrt{d^2 - |r\hat{R} + \hat{N} - \vec{O}|^2} \quad (68)$$

$$\hat{v} = \frac{r'\hat{R} + \hat{N} - \vec{O}}{d} \quad \blacksquare \quad (69)$$

$$m = \left( \frac{r' + |\vec{I}|}{\max(r' + |\vec{I}|)} \right)^2 \quad \blacksquare \quad (70)$$

Mirror dome projection perspective-map formula, where  $\vec{I}$  represents incident vector,  $\hat{N} \in [-1, 1]^3$  is the spherical-mirror world-normal and surface position,  $\vec{P}$  is the projector position,  $\vec{R}$  is reflection vector,  $r'$  is the reflection distance to dome intersection, as  $\hat{R} \cdot (\vec{O} - \hat{N}) = |\hat{R}| |\vec{O}'| \cos \alpha = 1 |\vec{O}'| r / |\vec{O}'| = r$ .  $\hat{v} \in [-1, 1]^3$  is the visual sphere vector as mirror surface color and  $\vec{O}$  is the dome origin position with  $d$  being dome radius. Mirror radius is equal 1 with its origin at position  $[0, 0, 0]$ . Light dimming mask is represented by  $m$  and it's based on inverse-square law approximation. In order to produce perspective map image, first mirror 3D model world-normal pass must be produced, as viewed from projector's perspective. It is possible to render the view with additional perspective map of the projector.

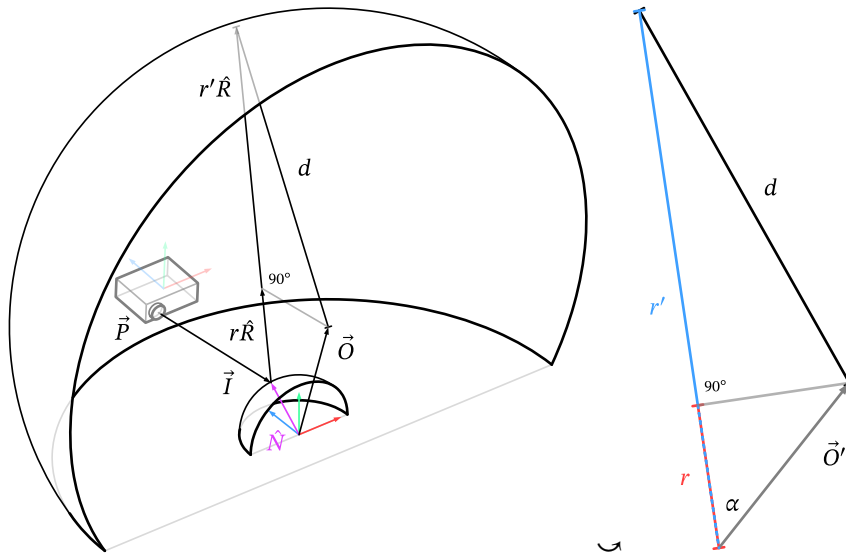


Figure 8: Mirror dome projection model, with mirror center as world origin.<sup>5</sup>

```

1 float dot(vec3 vector) { return dot(vector, vector); }
2 float sq(float scalar) { return scalar*scalar; }
3 float pxstep(float scalar)
4 { return clamp(scalar/fwidth(scalar), 0.0, 1.0); }
5
6 vec4 getMirrorDomeMap(vec3 mirror_normal, vec3 projector_map
7 , mat3 projector_rot, vec3 projector_pos, float
8 dome_radius, vec3 dome_pos)
9 {
10     vec3 reflection = reflect(projector_map, mirror_normal)*
11     projector_rot;
12     vec3 mirror_surface = mirror_normal*projector_rot;
13     dome_pos -= mirror_surface; // set current mirror surface as origin
14
15     // Get reflection length to dome intersection

```

```

13     float length = dot(reflection.xyz, dome_pos.xyz);
14     length += sqrt(sq(dome_radius)-dot(dome_pos.xyz-length*
      reflection.xyz) ));
15
16     return vec4(
17         (length*reflection.xyz-dome_pos.xyz)/dome_radius,
18         length+length(mirror_surface.xyz-projector_pos.xyz)
19     );
20 }
21
22 vec4 processMirrorDomeMask(vec2 tex_coord, vec3 dome_pos)
23 {
24     vec4 mirror_dome = texture2D(MirrorDomeMap, tex_coord);
25
26     // Get mirror-bounds mask
27     float alpha = texture2D(MirrorNormalPass, tex_coord).a;
28     // Generate reflected-dome-bounds mask
29     alpha *= pstep(mirror_dome.z); // half dome clip
30     alpha *= pstep(mirror_dome.y+dome_pos.y); // bottom clip
31
32     // Get maximum incident length for normalization
33     float max_incident = 0.0;
34     for (int y=0; y<sizeof(MirrorDomeMap).y; y++)
35     for (int x=0; x<sizeof(MirrorDomeMap).x; x++)
36         max_incident = max(
37             max_incident,
38             alpha*texture2D(MirrorDomeMap,
39                 vec2(x,y)/sizeof(MirrorDomeMap) ).w
40         );
41
42     // Combine normalized brightness mask
43     alpha *= sq(mirror_dome.w/max_incident);
44
45     return vec4(mirror_dome.xyz, alpha);
46 }

```

Listing 14: Mirror-dome visual-sphere vector  $\hat{v}$  from mirror normal-pass, as seen through projector in GLSL.

## 2.2.6 Projection mapping perspective map

$$\begin{bmatrix} \hat{v}_x \\ \hat{v}_y \\ \hat{v}_z \end{bmatrix} = \left\| \begin{matrix} \vec{S}_x - \vec{O}_x \\ \vec{S}_y - \vec{O}_y \\ \vec{S}_z - \vec{O}_z \end{matrix} \right\| \begin{bmatrix} O_{11} & O_{12} & O_{13} \\ O_{21} & O_{22} & O_{23} \\ O_{31} & O_{32} & O_{33} \end{bmatrix} \quad \blacksquare \quad (71)$$

$$m = \left( \frac{r}{\max r} \right)^2 \quad \blacksquare \quad (72)$$

Projection mapping perspective-map formula, where  $\hat{v}$  represents the visual

sphere vector as environment surface color,  $\vec{S}$  is the environment surface position,  $\vec{O}$  is the observation point position, with  $O$  as rotation matrix of the observation point  $\vec{O}$ .  $m$  is the light dimming mask based on inverse-square law, with  $r$  being the environment distance pass. In order to produce perspective map image, first environment 3D model pass must be produced representing world-position  $\vec{S}$ , as viewed from projector's perspective. It is possible to render the view with additional perspective map of the projector. More information about projection mapping is available in sub-subsection 1.1.5 on page 13.

```

1  float sq(scalar) { return scalar*scalar; }
2
3  vec3 getProjectionMap(vec2 tex_coord, vec3 view_pos, mat3
4  view_mat)
5  {
6      vec3 world_pos = texture2D(WorldPosPass, tex_coord).xyz;
7      return normalize(world_pos-view_pos)*view_mat;
8  }
9
10 float getBrightnessMask(vec2 tex_coord)
11 {
12     float max_distance = 0.0;
13     for (int y=0; y<sizeof(WorldPosPass).y; y++)
14         for (int x=0; x<sizeof(WorldPosPass).x; x++)
15             max_distance = max(
16                 max_distance,
17                 texture2D(WorldPosPass,
18                     vec2(x,y)/sizeof(WorldPosPass)).w
19             );
20     return sq(texture2D(WorldPosPass, tex_coord).w
21         /max_distance);
22 }

```

Listing 15: Visual sphere vector  $\hat{v}$  function from world-position pass as seen through projector in GLSL, for projection mapping.

## 2.2.7 Cube-mapping perspective map

$$\hat{X} = [1, 0, 0] \quad (73)$$

$$\hat{Y} = [0, 1, 0] \quad (74)$$

$$\hat{Z} = [0, 0, 1] \quad (75)$$

$$i = \left[ 6\vec{f}_s \right] \quad (76)$$

$$\begin{bmatrix} \hat{v}_x \\ \hat{v}_y \\ \hat{v}_z \end{bmatrix} = \left\| \begin{array}{c} (6\vec{f}_s) \bmod 1 - 1/2 \\ \vec{f}_t - 1/2 \\ 1/2 \end{array} \right\| \cdot \begin{cases} [\hat{Z}, -\hat{X}, -\hat{Y}], & \text{if } i = 0 \\ [-\hat{Z}, \hat{X}, -\hat{Y}], & \text{if } i = 1 \\ [\hat{X}, -\hat{Y}, -\hat{Z}], & \text{if } i = 2 \\ [\hat{X}, \hat{Z}, -\hat{Y}], & \text{if } i = 4 \\ [-\hat{X}, -\hat{Z}, -\hat{Y}], & \text{if } i = 5 \end{cases} \quad \blacksquare \quad (77)$$

Cube-mapping perspective-map formula, where  $\hat{v}$  represents visual sphere vector and  $\vec{f}$  are the screen coordinates.  $[\hat{Z}, -\hat{X}, -\hat{Y}]$  represents rotation matrix of each cube side. Operation  $x \bmod 1$  is equivalent to **fract**( $x$ ) function.

### 2.2.8 Multiple-screen array map

$$i = \lfloor n\vec{f}_s \rfloor + \frac{1-n}{2} \quad (78)$$

$$\begin{bmatrix} \hat{v}_x \\ \hat{v}_y \\ \hat{v}_z \end{bmatrix} = \left\| \begin{array}{c} 2((n\vec{f}_s) \bmod 1) - 1 \\ (2\vec{f}_t - 1)n \div a \\ \cot \frac{\Omega_h}{2} \end{array} \right\| \left\| \begin{array}{ccc} \cos(i\Omega_h) & 0 & \sin(i\Omega_h) \\ 0 & 1 & 0 \\ -\sin(i\Omega_h) & 0 & \cos(i\Omega_h) \end{array} \right\| \quad \blacksquare \quad (79)$$

$n$ -screen array perspective-map formula, where  $n$  is the number of screens,  $\hat{v}$  represents visual sphere vector,  $\vec{f}$  is the screen coordinates vector, with  $\Omega$  and  $a$  being a single-screen AOV and aspect ratio, respectively.

```

1  vec3 getScreenArrayMap(vec2 tex_coord , int n, float
   horizontal_fov , float aspect)
2  {
3      horizontal_fov = radians(horizontal_fov);
4      float index = floor(n*tex_coord.s)-0.5*n+0.5;
5      // Get single screen coordinates
6      vec3 direction = normalize(vec3(
7          2.0*fract(n*tex_coord.s)-1.0,
8          n*(2.0*tex_coord.t-1.0)/aspect ,
9          1.0/tan(horizontal_fov*0.5)
10     ));
11     // Rotate each screen individually
12     horizontal_fov *= index;
13     vec2 rotation = vec2(
14         sin(horizontal_fov) ,
15         cos(horizontal_fov)
16     );
17
18     return direction*mat3(
19         rotation[1], 0.0, rotation[0],
20         0.0, 1.0, 0.0,
21         -rotation[0], 0.0, rotation[1]
22     );

```

Listing 16: Visual sphere vector  $\hat{v}$  function from texture coordinates  $\vec{f}$  in GLSL, for  $n$ -screen array perspective.

### 2.2.9 VR perspective map

$$i = \text{sign}(\vec{f}_s - 1/2) \quad (80)$$

$$\begin{bmatrix} \vec{f}'_x \\ \vec{f}'_y \end{bmatrix} = \left( \begin{bmatrix} 2((2\vec{f}_s) \bmod 1) - 1 \\ 2\vec{f}_t - 1 \end{bmatrix} + \begin{bmatrix} i(1 - 2d) \\ 0 \end{bmatrix} \right) \begin{bmatrix} 0.5a \\ 1 \end{bmatrix} \quad (81)$$

$$\begin{bmatrix} \vec{f}''_x \\ \vec{f}''_y \end{bmatrix} = \begin{bmatrix} \vec{f}'_x \\ \vec{f}'_y \end{bmatrix} \frac{1 + k_1|\vec{f}'|^2 + k_2|\vec{f}'|^4 + \dots + k_n|\vec{f}'|^{2n}}{1 + k_1 + k_2 + \dots + k_n} \quad (82)$$

$$\begin{bmatrix} \hat{v}_x \\ \hat{v}_y \\ \hat{v}_z \end{bmatrix} = \begin{bmatrix} \vec{f}''_x \\ \vec{f}''_y \\ \cot \frac{\Omega_v}{2} \end{bmatrix} \quad \blacksquare \quad (83)$$

Virtual reality perspective map formula, where  $\vec{f}$  represents screen coordinates,  $d$  is the interpupillary distance (IPD) in screen-width scale,  $a$  is the screen aspect ratio,  $k_1, k_2, \dots, k_n$  represent lens-distortion coefficients.  $\hat{v}$  is the visual sphere vector and  $\Omega_v$  is the vertical AOV.

```

1  vec3 getVrMap(vec2 tex_coord, float ipd, float vertical_fov,
2  float k1, float k2, float aspect)
3  {
4  int index = sign(tex_coord.s - 0.5);
5  // Generate perspective coordinates
6  tex_coord.xy = 2.0 * vec2(fract(2.0 * tex_coord.s),
7  tex_coord.t) - 1.0;
8  tex_coord.x = (tex_coord.x + index * (1.0 - 2.0 * ipd)) * 0.5 *
9  aspect;
10 // Apply lens distortion
11 float R2 = dot(tex_coord, tex_coord);
12 tex_coord *= (1.0 + k1 * R2 + k2 * R2 * R2) / (1.0 + k1 + k2);
13
14 return normalize(vec3(
15     tex_coord,
16     1.0 / tan(radians(vertical_fov) * 0.5)
17 ));
18 }

```

Listing 17: VR visual-sphere vector  $\hat{v}$  from texture coordinates  $\vec{f}$  in GLSL. The **ipd** variable is expressed in screen-width scale.

### 2.3 Lens distortion of perspective picture

Creating perspective picture of a real optical system may require additional deformation of the vector data. Most commonly used algorithm is the *Brown-Conrady* lens distortion model.<sup>29</sup>

$$r^2 = \vec{f} \cdot \vec{f} \quad (84)$$

$$\vec{f}' = \begin{bmatrix} \vec{f}_x \\ \vec{f}_y \end{bmatrix} + (k_1 r^2 + k_2 r^4 + \dots + k_n r^{2n}) \begin{bmatrix} \vec{f}_x \\ \vec{f}_y \end{bmatrix} \quad \blacksquare \quad (85)$$

$$+ \left( \begin{bmatrix} p_1 \\ p_2 \end{bmatrix} \cdot \begin{bmatrix} \vec{f}_x \\ \vec{f}_y \end{bmatrix} \right) \begin{bmatrix} \vec{f}_x \\ \vec{f}_y \end{bmatrix} + \begin{bmatrix} q_1 r^2 \\ q_2 r^2 \end{bmatrix} \quad (86)$$

Where  $r$  is the dot product of two  $\vec{f}$  vectors.  $k_1, k_2$  and  $k_n$  are the radial distortion coefficients.  $q_1$  and  $q_2$  are the prism aberration coefficients. Misalignment coefficients are denoted by  $p_1$  and  $p_2$ .

*Remark.* Lens distortion vector is added to the view coordinates  $\vec{f}$  vector.

```

1  vec2 applyLensDistortion(vec2 tex_coord, float k1, float k2,
2     float p1, float p2, float q1, float q2, float aspect)
3  {
4     // Center coordinates, normalize diagonally
5     tex_coord.xy = 2.0*tex_coord.st - 1.0;
6     tex_coord /= length(vec2(aspect, 1.0) );
7     tex_coord.x *= aspect; // Correct aspect
8
9     vec2 distort_coord = tex_coord;
10    float R2 = dot(tex_coord, tex_coord);
11    // Radial distortion
12    distort_coord += tex_coord*(k1*R2+k2*R2*R2);
13    // Misalignment of lens
14    distort_coord += tex_coord*dot(vec2(p1, p2), tex_coord);
15    // Prism aberration
16    distort_coord += vec2(q1, q2)*R2;
17
18    return distort_coord;
19 }
```

Listing 18: Lens distortion function for transformation of view coordinates in GLSL.

## 3 No-parallax point mapping

Real optical systems exhibit phenomenon known as the floating no-parallax point,<sup>17</sup> where each portion of the picture represents different projection origin. To simulate such perspective, view position should change accordingly

to incident vector of given point, or in contrary, viewed point should move in the opposite way. In symmetrical lens, NPP offset is in  $z$ -direction and can be described as a product of function  $\text{parallax}(\theta)$ , as it changes accordingly to an incident angle from the optical lens center. Offset value can be approximated by optical measurement of parallax alignment (see figure 16 on page 44). To measure the origin point offset, first static NPP picture must be produced. If camera lens does not produce such image, it can be derived from a sequence of images, each taken at different  $z$  position (see subfigure 16d on page 44). Perspective vector map is derived from composite static NPP image. Offset value is mapped from sequence's source  $z$  position. To render picture with floating NPP, each 3D point must be transformed prior to rasterization, accordingly to perspective map position and associated offset value, either by moving the point or view position. The parallax offset values can also be encoded in a graph instead of texture map.

Rendering with rasterization would produce approximate result as values in-between vertices are not transformed accordingly to the parallax offset map. Therefore best quality floating-NPP result is achieved with ray-tracing. In such case, offset of ray-origin-position should be performed, which is equivalent to visual sphere origin offset (see subfigure 16b on page 44).

## 4 Appendix

Perspective picture visible inside the visual space gives some sense of immersion (e.g. picture, film, computer game) even without visual illusion.<sup>9</sup> That is because it's perceived as a visual symbol of an abstract point of view, through which not picture plane is seen, but depicted space mind-reconstruction. The picture immersion does not break, as long as objects appearance do not exhibit too much deformation. Perceiving abstract point of view invokes separation from the surrounding. To enhance immersion, environment stimuli is being reduced. In a movie theater, to uphold the immersion lights are turned off and silence is expected. Horror-gameplay session are usually played at night, to separate from safe-space of home. This approach focuses virtual presence on depicted space.

*Remark.* On the opposite side, picture as an integral part of the surrounding can be categorized under the *Trompe-l'œil* technique.<sup>28</sup>

Through the perception of the picture, physical properties of depicted space and objects within it are estimated. Mind fills the gaps, as symbols are always simplified versions of the real thing.

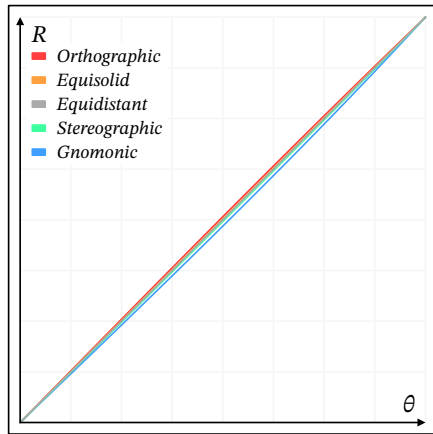
*Example.* Cup of coffee laying on a table has only one side visible at once, but it can be assumed that the opposite one is there too, since shape of the cup is known. This is a blank information filled by the mind.

Physical objects have their physical properties, but their visual symbols have some physical properties too, like angular size, perspective, shadow, etc. Those visual properties give some information about physical. In case of perspective,

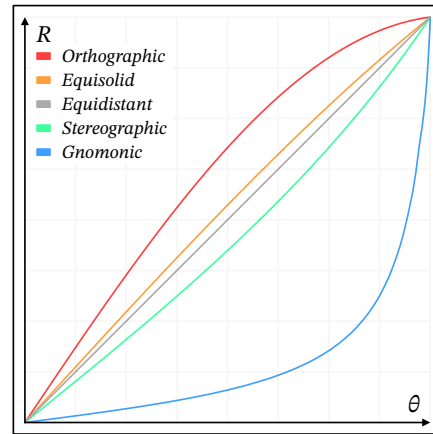
visual properties give information about depicted space and about point of view. Since most of the time picture presents a point of view (e.g. film, video game, visualization), it is wise to consider subject's properties of vision when designing picture's perspective. But instead of producing mechanical simulation, perspective should symbolize total sensory experience.<sup>2</sup>

**Theorem 1.** *To create immersive visual symbol of a visual space, it is necessary to use curvilinear perspective instead of a linear.*

*Proof.* Geometry of human visual space contradicts linear perspective principle, as visual field extends beyond linear perspective angle of view. Linear perspective, based on a tangent of an angle, exhibits limit of  $179.(9)8^\circ$  of view. While visual field extends horizontally up to  $220^\circ$  for binocular vision.<sup>15</sup> ■



(a) Graph plotting ray of angle  $\theta \in [0^\circ, \Omega]$  — as the horizontal axis, and screen-position radius  $R \in [0, 1]$ , as the vertical axis, where  $\Omega = 40^\circ$  which is equivalent to  $R = 1$ .



(b) Graph plotting ray of angle  $\theta \in [0^\circ, \Omega]$  — as the horizontal axis, and screen-position radius  $R \in [0, 1]$ , as the vertical axis, where  $\Omega = 170^\circ$  which is equivalent to  $R = 1$ .

Figure 9: Chart comparison of radial compression in five major azimuthal projections, across two different AOV ( $\Omega$ ) values: narrow (9a) and wide (9b).

At narrow AOV both types of perspective are suitable for immersive picture. In such case differences between each projection are negligible. Subfigure 9a presents those differences in comparison to five major perspective projections. Same differences seem exaggerated at higher AOV values (see subfigure 9b).

**Corollary 1.1.** *Practical limit for immersive picture in linear perspective is between  $60^\circ$  and  $110^\circ$  AOV. Wider-angles exhibit deformations known as the Leonardo Paradox,<sup>9</sup> which are then dominant in the image perception and break picture's immersion.* ■

To show wider-angle picture it is necessary to use curvilinear projection. But there is a tendency to see the world not through sight but understanding. We understand that the wall is flat, therefore we see it that way. Picture projected into the eye is just a visual symbol and has its own physical properties (e.g. perspective and shape). Therefore its visual representation is curvilinear, where the curvature symbolizes wider field of view. Reader can validate curvilinear nature of human visual space,<sup>4,11</sup> by following A. RADLEY experiment<sup>22</sup>:

*“Also when you have a moment, get a 30 cm ruler (...), and whilst looking forward bring it close to the bottom of your nose, and notice how its shape at the outer edges curves upwards and forwards. It may take you a few minutes to be able to see this effect, because you are so accustomed to not noticing it ! But once you do you will be amazed to see your curved field of view as it really is for the first time.” — A. RADLEY*

#### 4.1 Visual space symbolic picture

Since we came into conclusion that symbol of visual space is curvilinear, there is a choice between many non-linear projections. Each has properties that symbolize subject’s perception or information span about depicted space. Not appearance of the symbol should dominate the picture, but projected information about point of view and depicted space properties.

*Problem 1.* Which curvilinear perspective is best for visual symbol of visual space?

*Proposition 1.1.* A model based on anamorphic lens geometry; a mix between fish-eye, panini and anamorphic projection.

**fish-eye** as it can represent wider AOV than linear perspective (e.g.  $\pi$ ) and conforms to the curvilinear nature of VS. Gives natural spatial awareness.

**panini** to symbolize binocular vision; two spherical projections combined into one panoramic image.<sup>b</sup> Makes picture geometry more familiar to the viewer.

**anamorphic** as cylindrical projection, like *Panini*, tends to elongate proportions vertically; there is a need for correction. Correction should make object in focus proportional as it varies depending on position and size.

*Remark.* Only linear anamorphic correction will conform to the perspective picture definition (see on page 39).

*Remark.* Equations in subsection 2.1 on page 18 about perspective transformations present variables that manipulate all mentioned geometrical factors.

---

<sup>b</sup>Effect also referred as *Stereopsis*.

## 4.2 Visual sphere as a whole image

Common idea of an image is limited to a finite 2-dimensional plane. Which is subjective, due to constraints of human visual field and up-front placement of eyes. One can construct a rectangular frame, which at certain distance from the eyes will cover full visual field (VF). In case of some animals (e.g. horse, rabbit), visual space confines much wider VF. With only few blind spots, spanning to almost  $360^\circ$  AOV.<sup>3,18</sup> Such field cannot be enclosed by a single rectangular frame. Thus image nature is not of a frame. Another model has to be chosen instead. One able to cover full  $\Omega = 360^\circ$  is a sphere.

*Remark.* Cylindrical projection cannot cover full  $360^\circ$  AOV in all directions. It is a hybrid between frame and spherical model. When vertically-oriented, full  $\Omega_v < 180^\circ$ .

All three-dimensional space around given observation point, can be projected onto a sphere, with given observation point as origin. Even the sphere itself is a 3D object, its surface (as well as image nature)<sup>23</sup> is two-dimensional. Therefore creating perspective picture is a matter of representing portion of the visual sphere on a flat surface; a fundamental topic in cartography. Concept of a sphere as a model of visual space goes back as far as 300 BC, where Greek mathematician EUCLID seem first mentioning it (others are L. DA VINCI and F. AGUILONIUS).<sup>27</sup>

*Remark.* Each projection of sphere onto a flat surface is a compromise and can preserve only some properties (e.g. shape, area, distance or direction), which in case of perspective picture relates to some symbolic information about physical space.

**Definition 1.** Let us define perspective picture as the azimuthal projection, where lines converging at optical axis vanishing point remain straight, that *conservation of perspective* may occur (see definition on page 39).

### 4.2.1 Physical space properties preserved in azimuthal projections

Below are presented static properties of five major azimuthal projections. Properties of motion can be found in sub-subsection 4.3.2 on page 37. It is important to know which symbolic information about space is carried in each perspective projection, so that design choice for perspective geometry may be conscious.

**Gnomonic** (rectilinear) projects all great circles as straight lines, thus preserving directions. For 3D projection, straight lines in object-space remain straight. It does not preserve proportions, angles nor area or distances (see subfigure 10a on page 36). Extreme distortion occurs away from the center, in a form of a radial stretch (see *Leonardo Paradox*)<sup>9</sup>. AOV  $\Omega \in (0, \pi)$ .

*Example.* Most common perspective type in painting, 3D graphics and architectural visualization. Sometimes it is used to overemphasize building's appearance by leveraging *Leonardo Paradox*.<sup>9</sup> Wide AOV combined

with lowered optical center creates an effect of acute corners, producing extraordinary look. This technique may confuse the public, as symbolic picture experience won't match building's visual-space appearance.

**Stereographic** (conformal) preserves angles (at line intersection point). There is no perceivable radial compression, thus smaller figures retain their shape. It does not preserve distances (non-isometric), nor angular surface area. For 3D projection, most important factor is the conservation of proportions (see subfigure 10b on the following page). AOV  $\Omega \in (0, 2\pi)$ .

*Example.* In a picture with stereographic projection, actor's face keeps its shape and proportions, even at wide AOV. This projection gives also best spatial-awareness sensation (where visual cues are available). Good use case is for navigation through tight spaces and obstacles.

**Equidistant** preserves angular distance from the center point (see subfigure 10c on the next page). For 3D projection, angular speed of motion is preserved. Radial compression remains low-to-moderate at extreme  $\Omega$  angles. AOV  $\Omega \in (0, 2\pi]$ .

*Example.* This projection is recommended for target aiming or radar map navigation, where all targets are projected onto a Gaussian Sphere.

**Equisolid** preserves angular area. Gives good sensation of distance (see subfigure 10d on the following page). Radial compression is moderate up to  $\pi$ . Near maximum  $\Omega$ , compression is high. AOV  $\Omega \in (0, 2\pi]$ .

*Example.* When there are no spatial cues, this is best projection for putting emphasis on distance to the viewer.<sup>14</sup> Good use case is flight simulation, where only sky and other aircraft are in-view.

**Orthographic** preserves planar illuminance. It's a parallel projection of a visual hemisphere. Has extreme radial compression, especially near  $\pi$  (see subfigure 10e on the next page). AOV  $\Omega \in (0, \pi]$ .

*Example.* Most commonly found in very cheap lenses, like the peephole door viewer. Thanks to illuminance preservation, it is commonly used in sky photography.<sup>25</sup>

### 4.3 Image geometry and sensation of motion

Picture's perspective affects the way motion picture is perceived. It can enhance certain features, like proportions and shapes, movement or spatial-awareness. It can also guide viewer's attention to a specific region of image (e.g. center or periphery). Knowledge about these properties is essential for conscious image design.

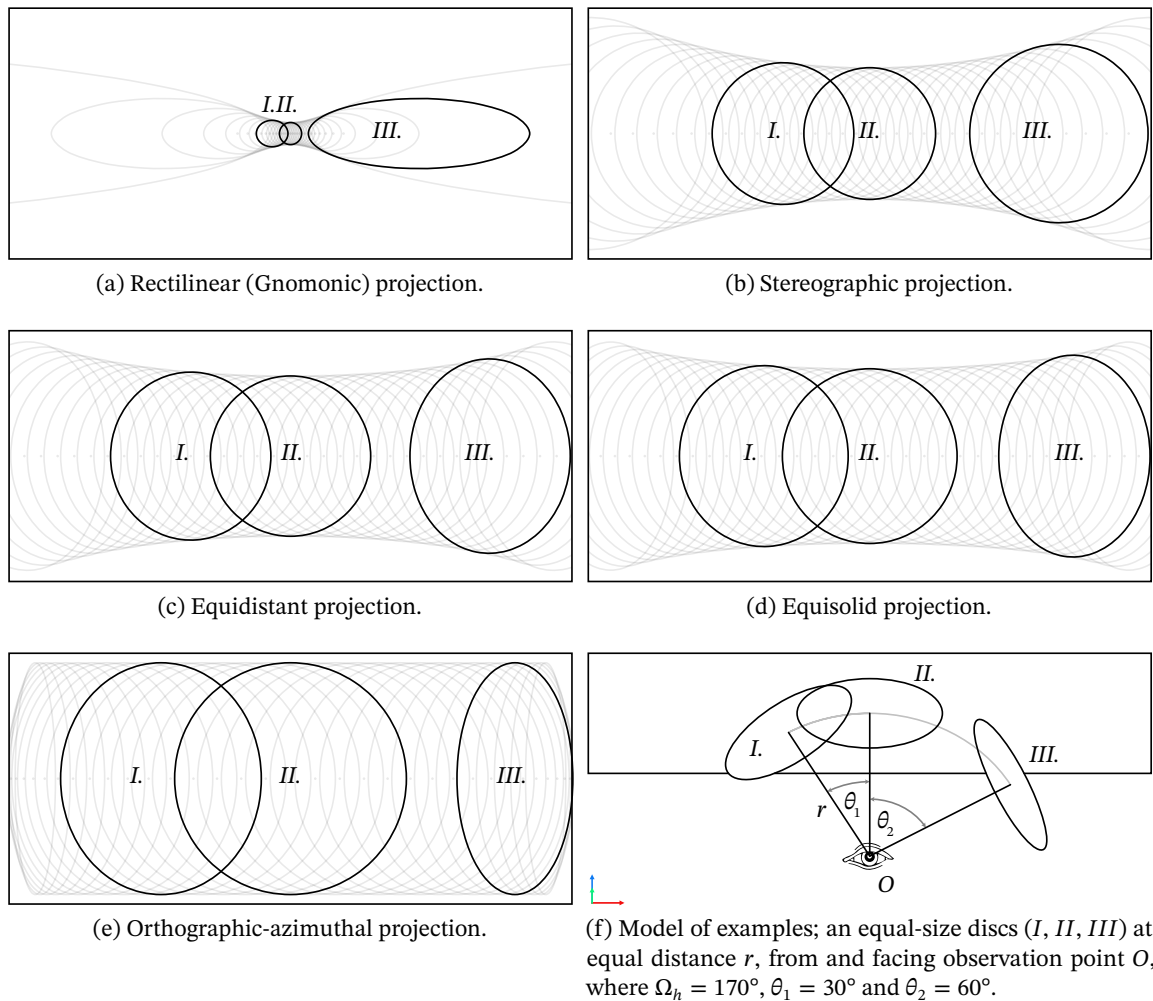


Figure 10: Example of motion in perspective picture in various azimuthal projections, where subfigure 10f presents viewed elements layout.

#### 4.3.1 Attention focusing

In film design, there are several techniques that focus viewer's attention on a specific portion of the picture, like *motion*, *color*, *light* and *composition*. Attention focusing through composition and motion is related to picture's perspective, as its geometry can compress and stretch the image. In composition, *rule of thirds* states that viewer's attention focuses on four corners of a rectangle produced by division of an image into three, equally-sized rows and columns. In motion, attention generally drives toward objects approaching the camera or those growing in scale. Attention also focuses on objects entering image frame. Same rules apply loosely in reverse, as attention suspense. Filmmakers tend to frame the image so that region of interest lays in accordance to the *rule of thirds*.

In case of computer games, region of interest is usually located at the very center, thus viewer must overcome the *principle of thirds* and some properties of *linear perspective* in order to switch attention to that region. In order to focus on the center, games usually incorporate some non-diegetic elements, like crosshair. Such approach may lower immersiveness of symbolic picture.<sup>6</sup>

#### 4.3.2 Attention focusing motion in perspective

Radial stretching and compression are the main attention focusing factors of perspective projection. They give subconscious sensation of movement towards camera, and can amplify figure's screen-relative speed of motion.

**Gnomonic** (rectilinear), due to extreme radial stretch, attention drives towards periphery. When approaching image bounds figures grow in scale and speed (see subfigure 10a on the preceding page). This combined with motion-sensitive peripheral vision adds to the effect. At wider AOV amplified motion breaks immersion of symbolic picture.

**Stereographic** also draws attention towards periphery. Figures grow in scale near bounds, but immersion does not break, as proportions are preserved, even at wide AOV (see subfigure 10b on the previous page).

**Equidistant** drives attention towards the center, as figures in periphery are radially compressed (see subfigure 10c on the preceding page). This projection preserves screen-relative, radial speed of motion, making it uniform and representative across the picture.

**Equisolid** also drives attention towards the center, as radial compression is even greater (see subfigure 10d on the previous page). Figure's speed of motion in screen-space slightly declines towards periphery.

**Orthographic** has extreme radial compression that breaks immersion of symbolic picture (see subfigure 10e on the preceding page). When in motion, image seem to be imposed on an artificial sphere.

*Gnomonic* and *Orthographic* projections are the two extremes of azimuthal spectrum. They are both least suited for an immersive picture. *Cylindrical* perspective type, while symbolizing binocular vision, also gives visual cues for the vertical axis orientation. Such cue is undesirable in case of camera roll motion, or when view is pointing up/down, as image vertical axis will not align with depicted space orientation. In such case perspective geometry should transition from *panini* to *spherical* projection (see figure 11 on the next page).

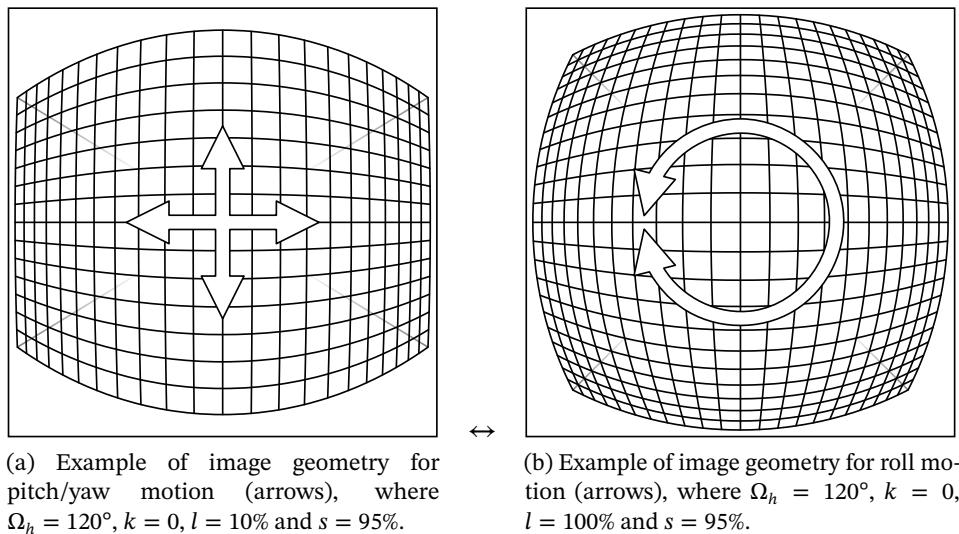


Figure 11: Examples of image geometry for a given view-motion type.

#### 4.4 History of the topic and previous work

Current image abstract theorem was established in 15<sup>th</sup> century book *De Pictura*, by L. B. ALBERTI. Based on invention of F. BRUNELLESCHI, ALBERTI defined geometrical and theoretical rules for designing perspective projections.<sup>2</sup> Those rules are currently used in polygon-based CG graphics. Major theoretical statement that laid foundation for image projection technology and present understanding of image nature can be traced back to ALBERTI abstract definition of image. He would describe a painting to be like a window in a wall<sup>1</sup>:

*“First of all, on the surface on which I am going to paint, I draw a rectangle of whatever size I want, which I regard as an open window through which the subject to be painted is seen.”* — L. B. ALBERTI

But in times of its discovery, as for now, linear perspective introduced itself with several issues. When there’s a need for a wide-angle view, one close to the human visual field, geometrical distortions appear to dominate visual aspect of the picture. Those issues were noticed by Renaissance artists, like L. DA VINCI. He put to the test the Alberti Theorem and produced paintings of accurate-perspective.<sup>7</sup> In his *Treatise on Painting*, DA VINCI notes that picture conforms to the idea of a window only when viewed from one specific point in space.<sup>8</sup> Stating that seen otherwise, objects appear distorted, especially in the periphery. Picture then, viewed from a different point ceases to be like a window in a wall and becomes a visual symbol of an abstract point of view.<sup>c</sup> Some 18<sup>th</sup> century late Baroque and Neoclassical artists, when encountered these issues,

<sup>c</sup>Effect also referred to *Zeeman Paradox*.<sup>9</sup>

introduced derivative projections. Like G. P. PANNINI with later re-discovered *Panini Projection*,<sup>21</sup> or R. BARKER, who established the term *Panorama*.<sup>30</sup> This was a new type of perspective. A form of cylindrical projection, where abstract window frame becomes horizontally curved, reducing deformation artifacts in wide, panoramic depictions of architecture.



Figure 12: Still from TODD-AO HIGH-SPEED ANAMORPHIC lens (35mm T1.4) with visible curvilinear perspective. This type of lens was featured in films like *Conan the Barbarian*, *Dune* and *Mad Max*.<sup>26</sup>

© 2017 ShareGrid, Inc.

**Invention of motion picture** followed by the rise of film industry, resulted in demand for a new image geometry. Previously still, now pictures had to be pleasing to the eye, in motion. 1950s brought anamorphic cinematography to the wider audience. Lenses like CINEMASCOPE and later PANAVISION<sup>16</sup> became standard in film production. Figure 12 shows example of mixed spherical and cylindrical projection in anamorphic lens, with perspective preservation.

**Definition 2.** *Conservation of perspective* - lines converging at the optical-axis vanishing-point remain straight.

*Remark.* See also perspective picture definition on page 34.

CG image technology did not follow film industry in that field. Still based on Alberti Theorem, computer graphics became incompatible with film, generating great costs, when two had to be joined together.<sup>24</sup> Which is mostly due to lens aberration rotoscoping, where geometry correction has to be performed manually for each frame. Currently in computer-games industry, CG imagery is practically unable to produce realistic, curvilinear simulation of visual space (VS), or even simulate anamorphic lens geometry, due to limits of linear perspective and resource costs of overcoming those issues. Some hybrid solutions for real-time graphics were proposed,<sup>13,14</sup> that combine rasterization with ray-tracing, or tessellation. Such approach allows for a semi-practical and limited production of real-time pictures in a non-linear perspective.

## 5 Conclusion and future work

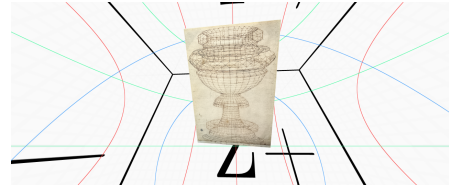
Visual sphere perspective model expands possibilities for image creation. Like a vision of a classical artist is richer and more dynamic than his final creation, so should be a model describing image. So much that virtual vision would have to be reduced to fit the medium, with additional room for adjustment.

In medieval times people were fascinated with mirror, it depicted reality as it really is, a task impossible for human hand. But mirror could not reflect the vision of imagination, so much as painting. It did not produce realistic reflection of reality, nor reflection of imagination. In art there was a pursuit involving philosophy and religion to reach some imaginary reflection. Only after BRUNELLESCHI experiment proved that painting created by human hand, with strict rules of geometry, reflected from a mirror fits well into reality, artists started pursuing mathematics of art. Film and photography became a new mirror, but still not one of imagination. Finally computer graphics became a format capable to reflect one's vision of imagination, but struggled to be photo-real.

Language of image is ultimately a language of symbols, it works in conjunction with mind which recreates visual space of the picture. Computer game's image is different from one of film in a sense that rather being a viewing glass it impersonates point of view of the protagonist, which invokes different symbolic measures. Real-time graphics should be capable to incorporate such symbols in the result. One way for achieving this is to switch perspective model for a bigger one. Proposed switch includes use of universal perspective model which defines simple variables for manipulation of perspective geometry. It also includes production technique for a real-time imagery using this model. This new solution fits well into current graphics pipeline, replacing only low-level rasterization processes. Aliasing-free end result is comparable in quality to  $8 \times$  MSAA and enables previously impossible visual effects in real-time graphics. Presented visual sphere model unites all types of perspective projections under one technical solution, making perspective a fluid construct. Perspective vector maps can be easily combined and transformed by spherical interpolation. Picture geometry can now be designed to smoothly adapt to the visual story, giving new dimension of control over mental perception of image. Presented concepts and equations may also find their use in other fields, not rendering-related. This is a great base as well as complete solution upon which many new technologies and works can emerge. Some specific use cases still require additional research, like hidden surface removal and no-parallax point mapping. Further studies will include research over calibration and simulation of real optical systems with floating NPP. Also performance tests, comparison to current solutions should be evaluated by future research. Psychological analysis of perspective geometry magnitude of influence on depicted space perception, performed on a large sample data, could be an interesting field to study.



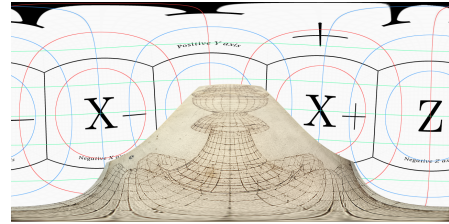
(a) Rectilinear perspective, where  $\Omega_d = 140^\circ$ ,  $k = 1, l = 1$ . *Vector map*.



(b) Rectilinear perspective, where  $\Omega_d = 140^\circ$ ,  $k = 1, l = 1$ . *Rasterized quad*.



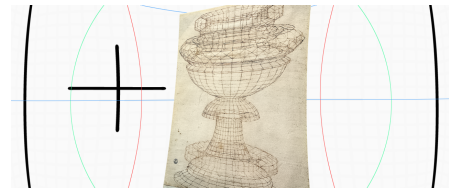
(c) Equirectangular projection of a whole sphere, where  $\Omega_h = 360^\circ$  and  $\Omega_v = 180^\circ$ . *Vector map*.



(d) Equirectangular projection, where  $\Omega_h = 360^\circ$  and  $\Omega_v = 180^\circ$ . *Rasterized quad*.



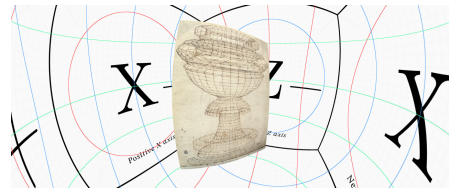
(e) Mustache-type lens distortion, where  $\Omega_d = 131^\circ$ ,  $k = 0.32, l = 62\%, s = 86\%$ ,  $k_1 = -0.6, k_2 = 0.4$ . *Vector map*.



(f) Mustache-type lens distortion, where  $\Omega_d = 131^\circ$ ,  $k = 0.32, l = 62\%, s = 86\%$ ,  $k_1 = -0.6, k_2 = 0.4$ . *Rasterized quad*.



(g) Curvilinear fish-eye perspective, where  $\Omega_d = 270^\circ$ ,  $k = 0.32, l = 62\%, s = 86\%$ . *Vector map*.



(h) Curvilinear fish-eye perspective, where  $\Omega_d = 270^\circ$ ,  $k = 0.32, l = 62\%, s = 86\%$ . *Rasterized quad*.



(i) Five-screen horizontal array in rectilinear projection, where single screen  $\Omega_{h,v} = 60^\circ$ ,  $k = 1$  and  $l = 1$ , giving a total  $5\Omega_h = 300^\circ$ . *Vector map*.



(j) Five-screen horizontal array, where single screen  $\Omega_{h,v} = 60^\circ$ ,  $k = 1$  and  $l = 1$ , giving a total  $5\Omega_h = 300^\circ$ . *Rasterized quad*.

Figure 13: Examples of polygon quad rasterization directly from three-dimensional space to the image, using visual-sphere vector map  $G$ , where  $G_{st}^{\vec{s}} \in [0, 1]^3 \leftarrow [-1, 1]^3$ .



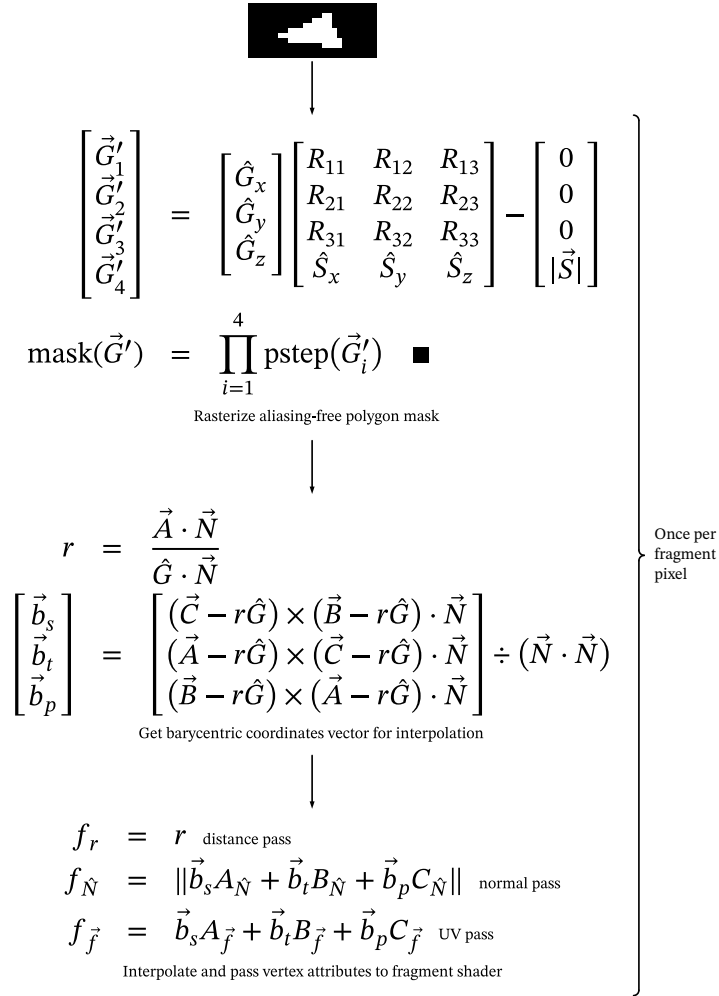
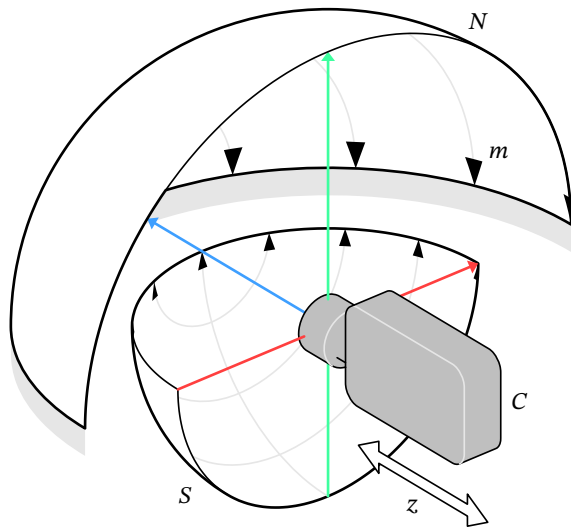
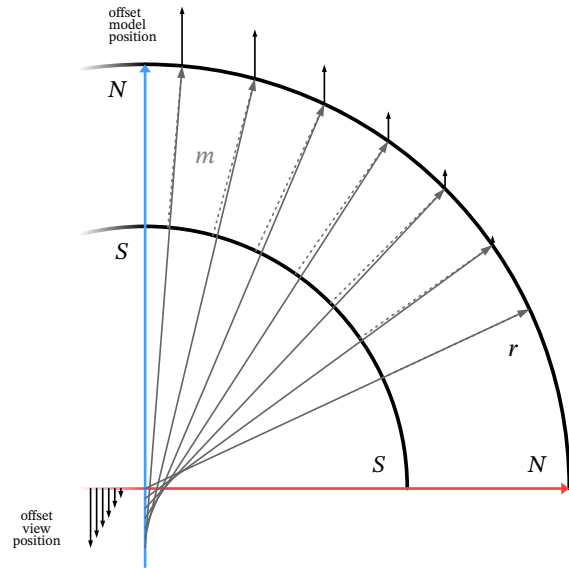


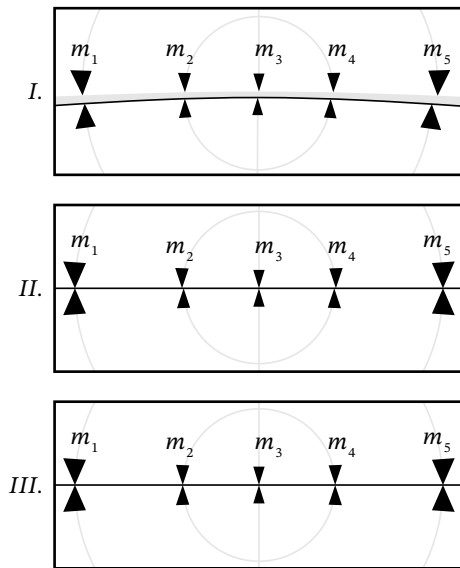
Figure 15: Fragment rasterization process flowchart which starts with rasterization matrix  $R'$ , binary mask of render regions, polygon normal vector  $\vec{N}$ , triangle points  $\vec{A}, \vec{B}, \vec{C}$  and perspective vector map  $\vec{G}$ . For each pixel, aliasing-free mask is produced and barycentric coordinates  $\vec{b}$  are calculated, then interpolated vertex data  $f$  is passed to fragment shader as output.



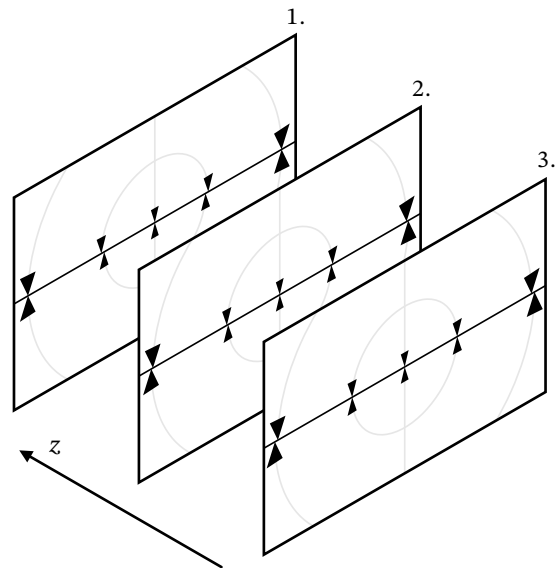
(a) Model of no-parallax point (NPP) calibration rig. Which measures misalignment of  $m$  markers between northern ( $N$ ) and southern hemisphere ( $S$ ), as seen through camera  $C$ .



(b) Simulation of floating NPP in fish-eye camera. Black arrows represent position offset of the model for rasterization and view position offset for ray-tracing. When measuring the NPP (sub-figure 16c), camera travel is opposite to view position offset.



(c) Example *I* presents misalignment of the camera in all three axes. Example *II* presents alignment in X, Y axis, where peripheral marker pair  $m_1, m_5$  present alignment near horizontal AOV, while pairs  $m_2, m_4$  are misaligned due to floating NPP. Example *III* presents "slit-scan" composite of variable  $z$  position, where all markers are aligned.



(d) Example of a variable camera position  $z$  encoded in an image sequence (1, 2, 3). Element 1 presents alignment of the peripheral markers, while element 3 presents alignment of the side markers, element number 2 presents position in-between.

Figure 16: Floating no-parallax point rendering and measurement process.

## References

1. Alberti, L. B. in *On painting and on sculpture* trans. by Grayson, C., 55 (Phaidon, London, England, 1972). [http://as.vanderbilt.edu/koepnick/Modernism\\_f05/materials/images/alberti\\_window.htm](http://as.vanderbilt.edu/koepnick/Modernism_f05/materials/images/alberti_window.htm) (cit. on p. 38).
2. Argan, G. C. & Robb, N. A. The Architecture of Brunelleschi and the Origins of Perspective Theory in the Fifteenth Century. *Journal of the Warburg and Courtauld Institutes* **9**, 96. doi:10.2307/750311 (1946) (cit. on pp. 32, 38).
3. Bagley, L. H. & Lavach, D. in Varga, M. *Textbook of Rabbit Medicine E-Book* chap. 9.1 Ocular anatomy and physiology (Butterworth-Heinemann, 2013) (cit. on p. 34).
4. Baldwin, J., Burleigh, A. & Pepperell, R. Comparing Artistic and Geometrical Perspective Depictions of Space in the Visual Field. *i-Perception* **5**, 536–547. doi:10.1068/i0668. <http://journals.sagepub.com/doi/pdf/10.1068/i0668> (2014) (cit. on p. 33).
5. Bourke, P. Low Cost Projection Environment for Immersive Gaming. *Journal of MultiMedia* **3**, 41–46. doi:10.4304/jmm.3.1.41-46. <http://paulbourke.net/papers/dime2006/dime2006.pdf> (2008) (cit. on pp. 24, 25).
6. Casamassina, M. *King Kong's Immersive Style* IGN. <http://ign.com/articles/2005/07/18/king-kongs-immersive-style> (2019) (cit. on p. 37).
7. Da Vinci, L. *Annunciation* oil and tempera on panel. Painting. Uffizi Gallery, Florence, Italy, 1475-1480. [http://en.wikipedia.org/wiki/De\\_pictura#/media/File:Leonardo\\_Da\\_Vinci\\_-\\_Annunciazione.jpeg](http://en.wikipedia.org/wiki/De_pictura#/media/File:Leonardo_Da_Vinci_-_Annunciazione.jpeg) (cit. on p. 38).
8. Da Vinci, L. in *A treatise on painting* trans. by Rigaud, J. F., 52 (Project Gutenberg, Salt Lake City, USA, 2014). <http://gutenberg.org/ebooks/46915> (cit. on p. 38).
9. Dixon, R. in *Mathographics* 82–83 (Dover Publications, Great Britain, 1987) (cit. on pp. 31, 32, 34, 38).
10. Ericson, C. *Minimum bounding circle (sphere) for a triangle (tetrahedron)* <http://realtimecollisiondetection.net/blog/?p=20> (2020) (cit. on p. 7).
11. Erkelens, C. J. The Perspective Structure of Visual Space. *i-Perception* **6**. doi:10.1177/2041669515613672. <http://journals.sagepub.com/doi/pdf/10.1177/2041669515613672> (2015) (cit. on p. 33).

12. Fuchs, H., Kedem, Z. M. & Naylor, B. F. *On visible surface generation by a priori tree structures* in *Proceedings of the 7th annual conference on Computer graphics and interactive techniques - SIGGRAPH 80* (ACM Press, 1980). doi:10.1145/800250.807481 (cit. on p. 17).
13. Gascuel, J.-D., Holzschuch, N., Fournier, G. & Péroche, B. *Fast Non-linear Projections Using Graphics Hardware* in *ACM Symposium on Interactive 3D Graphics and Games* (ACM, Redwood City, California, 2008), 107–114. doi:10.1145/1342250.1342267. <http://maverick.inria.fr/Publications/2008/GHFP08/i3d2007.pdf> (cit. on p. 39).
14. Glaeser, G. & Gröller, E. Fast generation of curved perspectives for ultra-wide-angle lenses in VR applications. *The Visual Computer* **15**, 365–376. doi:10.1007/s003710050185 (1999) (cit. on pp. 35, 39).
15. Hueck, A. *Von den Grenzen des Sehvermögens* ger, 84. [http://hans-strasburger.userweb.mwn.de/materials/hueck\\_1840\\_ocr.pdf](http://hans-strasburger.userweb.mwn.de/materials/hueck_1840_ocr.pdf) (Müller's Archiv, Tartu, 1840) (cit. on p. 32).
16. Königsberg, I. *The complete film dictionary* 12. <http://archive.org/details/completefilmdict00koni> (Nal Penguin INC, New York, USA, 1987) (cit. on p. 39).
17. Littlefield, R. Theory of the No-Parallax Point in Panorama Photography. <http://janrik.net/PanoPostings/NoParallaxPoint/TheoryOfTheNoParallaxPoint.pdf> (2006) (cit. on p. 30).
18. Miller, P. E. & Murphy, C. J. in *Equine Ophthalmology* (ed Gilger, B. C.) chap. Visual perspective and field of view (Elsevier Health Sciences, St. Louis, USA, 2010) (cit. on p. 34).
19. Muszyński, G., Guzek, K. & Napieralski, P. *Wide Field of View Projection Using Rasterization* in *Multimedia and Network Information Systems* (eds Choroś, K., Kopel, M., Kukla, E. & Siemiński, A.) (Springer International Publishing, Cham, 2019), 586–595. doi:10.1007/978-3-319-98678-4\_58 (cit. on p. 4).
20. Newell, M. E., Newell, R. G. & Sancha, T. L. *A solution to the hidden surface problem* in *Proceedings of the ACM annual conference on - ACM72* (ACM Press, 1972). doi:10.1145/800193.569954 (cit. on p. 17).
21. Pannini, G. P. *Interior of St. Peter's* oil on canvas. Painting. National Gallery of Art, Washington DC, USA, 1754. <http://web.archive.org/web/20130327080328/vedutismo.net/Pannini/> (cit. on p. 39).
22. Radley, A. in Cipolla-Ficarra, F. V. *Handbook of Research on Interactive Information Quality in Expanding Social Network Communications* 46 (IGI Global, 2015). <http://books.google.com/books?id=90yfBwAAQBAJ> (cit. on p. 33).

23. Rybczyński, Z. *a Treatise on the Visual Image* (ed Oszmiańska, H.) chap. 1.2.2. <http://books.google.com/books?id=mUHNAQAACAAJ> (Art Stations Foundation, Poznań, Poland, 2009) (cit. on p. 34).
24. Rydzak, J. *Zbig Rybczyński, Oscar-Winning Filmmaker* interview. Arizona, USA, 2014. [http://youtube.com/watch?v=071\\_XgZ4{H}2I](http://youtube.com/watch?v=071_XgZ4{H}2I) (cit. on p. 39).
25. Thoby, M. *About the various projections of the photographic objective lenses. Orthographic fisheye projection* [http://michel.thoby.free.fr/Fisheye\\_history\\_short/Projections/Variou\\_lens\\_projection.html](http://michel.thoby.free.fr/Fisheye_history_short/Projections/Variou_lens_projection.html) (2019) (cit. on p. 35).
26. *Todd AO High-Speed Anamorphic 35mm T1.4 at T2.0log* from The Ultimate Anamorphic Lens Test. ShareGrid, Inc. <https://learn.sharegrid.com/sharegrid-lens-test-todd-ao-anamorphic> (2020) (cit. on p. 39).
27. Tyler, C. W. Straightness and the Sphere of Vision. *Perception* **38**, 1423–1427. doi:10.1068/p3810ed (2009) (cit. on p. 34).
28. Wade, N. J. & Hughes, P. Fooling the Eyes: Trompe LOeil and Reverse Perspective. *Perception* **28**, 1115–1119. doi:10.1068/p281115. [http://wexler.free.fr/library/files/wade%20\(1999\)%20fooling%20the%20eyes.%20trompe%20oeil%20and%20reverse%20perspective.pdf](http://wexler.free.fr/library/files/wade%20(1999)%20fooling%20the%20eyes.%20trompe%20oeil%20and%20reverse%20perspective.pdf) (1999) (cit. on p. 31).
29. Wang, J., Shi, F., Zhang, J. & Liu, Y. A new calibration model of camera lens distortion. *Pattern Recognition* **41**, 607–615. doi:10.1016/j.patcog.2007.06.012. <http://dia.fi.upm.es/~lbaumela/Vision13/PapersCalibracion/wang-PR208.pdf> (2008) (cit. on p. 30).
30. Wikipedia, c. *Robert Barker (painter)*. *Biography* Wikipedia, The Free Encyclopedia. [http://en.wikipedia.org/w/index.php?title=Robert\\_Barker\\_\(painter\)&oldid=907715733#Biography](http://en.wikipedia.org/w/index.php?title=Robert_Barker_(painter)&oldid=907715733#Biography) (2019) (cit. on p. 39).

© 2020 Jakub Maksymilian Fober (the Author). The Author provides this document (the Work) under the Creative Commons CC BY-ND 3.0 license available online. To view a copy of this license, visit <https://creativecommons.org/licenses/by-nd/3.0/> or send a letter to Creative Commons, PO Box 1866, Mountain View, CA 94042, USA. The Author further grants permission for reuse of images and text from the first page of the Work, provided that the reuse is for the purpose of promoting and/or summarizing the Work in scholarly venues and that any reuse is accompanied by a scientific citation to the Work.

